2012

Investigation of biomass gasification and effects of ammonia on producer gas combustion

Jordan A. Tiarks
Iowa State University

Investigation of biomass gasification and effects of ammonia on producer gas combustion

by

Jordan Alan Tiarks

A thesis submitted to the graduate faculty

in partial fulfillment of the requirements for the degree of

MASTER OF SCIENCE

Major: Mechanical Engineering

Program of Study Committee:
Song-Charng Kong, Major Professor
Terrence Meyer
James Hill

Iowa State University

Ames, Iowa

2012

TABLE OF CONTENTS

LIST OF FIGURES

LIST OF TABLES

ACKNOWLEDGEMENT

Many people have invested a great deal of time, energy, and talent in supporting me in this research. I thank Dr. Song-Charng Kong for giving me the opportunity to work on a project that has been of great interest and benefit to me. He has provided continued guidance and support throughout my Master's program at Iowa State University and his encouragement has helped me along this journey. I would like to thank Dr. Terrence Meyer for his support and guidance throughout the experimental portion of this work and overall Master's program. I would also like to thank Dr. James Hill for serving as my committee member.

A great deal of assistance has been provided to me by the staff in the Department of Mechanical Engineering. I thank Deb Schroeder, Carol Knutson and Jim Dautremont for their administrative and technical support throughout this project.

My fellow graduate students and group members have provided valuable help and discussion throughout this program. I would like to thank the members of Dr. Kong's and Dr. Meyer's group for making this work enjoyable and for providing guidance and support along the way. In particular, I thank Cuong Van Huynh, Sudhanya Banerjee, Sujith Sukumaran, Christopher Gross, George Zacharakis-Jutz, Praveen Kumar, Miao Li, Yanan Zhang, and Lowell Stutzman for all you have done.

Finally, I would like to thank my family and friends for all of their support. To my parents – The sacrifices you have made and the love and encouragement you have given to me have provided a world of possibilities and have helped me become the person I am today. From the bottom of my heart, thank you for all you have done.

ABSTRACT

Energy security and global climate change are two of the greatest challenges that face the next century and it will be up to this generation to figure out a solution to these monumental challenges. Nearly everything ranging from commerce to travel to education relies on abundant and cheap energy to function and progress. For the last 150 years, this energy has come through the combustion of fossil fuels which are limited by their very nature. As these fuels are combusted to produce heat and power, various harmful gasses are emitted into the atmosphere and can lead to "acid rain," smog, depletion of the ozone layer, and even a heating of the earth's surface. Gasification of biomass provides one possible solution to both of these problems by utilizing a renewable energy source that is abundant and has the potential to be carbon negative. NO_x emissions are regulated by the government and could potentially be the limiting factor on the potential of biomass gasification to have a major impact in overcoming the two greatest challenges of today. It is believed one of the primary causes of NO_x emissions is due to nitrogen found in the feedstock that is gasified. This work is aimed at both developing the tools necessary to understand the detailed systems involved in biomass gasification, as well as to characterize the NO_x emissions that result from the combustion of the biomass-derived producer gas.

In the current work, a two-fold approach is taken to address this issue. First, a process model is created utilizing the software Aspen Plus to simulate data taken from a pilot-scale gasification system utilizing maple and oak wood as the feedstock and air as the gasification medium. This model uses a mass balance approach to

simulate the gasification process. A system of cyclones filter out the particulate matter in the producer gas before the gas is burned. Second, the effects of fuel-NO_x are studied experimentally utilizing a newly developed lab-scale, low-swirl combustion apparatus. This combustion apparatus is first tested using natural gas that contains low concentrations of ammonia for four swirlers with varying effective areas. A single swirler is chosen to conduct tests to analyze the effect of ammonia concentration on NO_x emissions from the producer gas.

Results of the current work can be summarized as follows. (1) A biomass gasification model was created to model the gasification of wood feedstock. This model shows very good agreement with experimental results for all components except hydrogen in the producer gas. (2) For the swirlers studied, NO_x emissions are reduced as the swirl strength increases. (3) For a natural gas flame, both the equivalence ratio and effect of thermal NO_x are important considerations when trying to achieve low NO_x emissions. (4) For the combustion of producer gas, higher equivalence ratios reduce the overall NO_x emissions. The above results show the need for a greater understanding of producer gas combustion in low-swirl burners for a wide variety of compositions in order to better control overall emissions in the future.

CHAPTER 1. INTRODUCTION

1.1 Motivation

According to the Energy Information Administration, the renewable energy sector is projected to be the fastest growing area of energy consumption for the years ranging from 2009 to 2035. In this sector, total biomass energy consumption is projected to grow at a rate of 2.9% per year with specific areas growing at even higher rates including electricity generation growing by up to 5.6% per year (EIA, 2011). This rapid growth can be attributed to a wide variety of causes including new policy decisions that have shaped the future energy market, economic uncertainty in the last decade, and growing environmental concerns due to greenhouse gas (GHG) emissions. Since the oil crisis of the 1970s, experts in US energy have agreed that the nation's dependence on oil exposes its economy to high instabilities and puts national security at increased risks (Greene, 2010). Coupling this fact with increasing concerns over global warming has led to new national and state policies that have aimed at increasing renewable energy usage in the United States and reducing the dependence on fossil fuels. In 2009, the EPA issued a revised Renewable Fuel Standard (RFS2) that set increased minimum biorenewable transportation fuel mandates through the year 2022. Additionally, in order to qualify as a renewable fuel, life cycle analysis of each type of fuel must confirm that the renewable fuel produces a net reduction in GHG emissions, with different benchmarks for type of fuel and amount of GHG reduction (EPA, 2010). This policy means that methods of energy generation now play a significant role in the net

benefit from a given biofuel, and some ethanol refineries that gain electricity and process heat from coal would no longer qualify as a renewable fuel. Finally, at the time of writing this thesis, the EPA has proposed a new carbon pollution standard (expected to become a policy) for all future new power plants that calls for a 50% reduction in carbon emissions from coal fired power plants. This effectively limits new power plants to be based on natural gas or other clean energy sources such as biomass (EPA, 2012).

Biomass gasification is one of the technologies currently being investigated which could show great promise in meeting the environmental, economic, and policy concerns of the current decade and into the future. Biomass gasification is a thermo-chemical process that generates producer gas or synthesis gas when the biomass feedstock is exposed to a high temperature, fuel rich environment in the presence of air, steam, and/or oxygen as a fluidizing agent (Li, et al., 2004). Air blown gasification produces a low calorific value gas called a "producer gas," with higher heating values (HHV) between 4 to 7 MJ/Nm^3 while oxygen and steam gasification producer a medium calorific value gas called "synthesis gas," which has a HHV between 10 to 18 MJ/Nm^3 (Li, et al., 2000). Comparatively, natural gas has a HHV of 36 MJ/Nm^3. Note that the subject of this research is based on air-blown gasification so the term "producer gas" will be used in this thesis. Depending on the heating value and properties of the gas, end use potential ranges from process heat and energy generation on the low end, to chemical and fuel synthesis via catalytic reforming on the high end (Kirkels, et al., 2011).

As has been stated, one of the benefits of biomass gasification is the low net emissions of GHGs, namely carbon dioxide, into the environment when compared to other energy sources. The drawback however is that nitrogen found in the biomass is passed on to the producer gas and results in greater NO_x emissions when combusted. Work has been done to classify the effects of fuel bound nitrogen (FBN) to producer gas composition and combustion emissions ((Zhou, et al., 2000), (Tian, et al., 2007), (Sethuraman, et al., 2011)). It has been shown that nitrogen in the biomass feedstock is converted to various nitrogen containing compounds in the producer gas including elemental nitrogen (N_2), ammonia (NH_3), and hydrogen cyanide (HCN) depending on the conditions of the gasifier. Of the nitrogen containing species, ammonia is the dominant compound in producer gas and contributes most significantly to fuel NO_x when combusted in a burner or internal combustion engine (Tian, et al., 2007). Study of NO_x emissions from the combustion of ammonia containing producer gas has shown a direct relationship between NO_x emissions and ammonia concentration in the producer gas (Sethuraman, et al., 2011). Additional investigations into the combustion of ammonia containing producer gas at additional operating conditions are needed.

Modeling of biomass gasification has been a subject of great effort for over a decade. Methods of modeling gasification include kinetic rate models, thermodynamic equilibrium models, and neural network models. Due to the complexity in gasification zones as well as the wide spectrum of biomass feedstocks used in gasification, no model has yet proven itself as a leader in the field (Puig-

Arnavat, et al., 2010). Thermodynamic models allow for preliminary comparison of operating conditions and feedstock types while being limited in their ability to give accurate and detailed information. Kinetic based models provide a greater level of accuracy yet are limited to the feedstocks they can predict. Therefore, models must be customized for different reactor configurations and feedstocks in order to be of the most benefit to site specific analysis.

1.2 Objective

The objective of this work is to model a biomass gasification system and characterize effects of ammonia on producer gas combustion. It is believed that ammonia levels in producer gas are proportional to the nitrogen content in the feedstock. In turn, higher ammonia levels are believed to contribute to higher NO_x emissions due to the fuel NO_x pathway (Li, et al., 2000). The goal of this research is twofold. This study will develop a gasification model based on Aspen Plus which can be tailored to model various feedstocks. Additionally, laboratory scale combustion tests will also be conducted in order to characterize NO_x emissions for the combustion of producer gas seeded with varying levels of ammonia.

CHAPTER 2. LITERATURE REVIEW

2.1 Biorenewable Resources

Throughout the majority of human history, biorenewable resources served as the foundation on which many of the advancements in early human society including foodstuffs, fire, tools, and even clothing can be attributed. Reliance on biorenewable resources in society continued until relatively recent times when coal and other fossil fuels gained dominance for providing energy and eventually chemicals and fibers, starting in the mid-eighteenth century. These biorenewable resources are defined as “organic materials of recent biological origin” which are “sustainable and available for use by future generations” (Brown, 2003). Included in the biorenewable resource base are energy resources including agricultural and forestry residues, energy crops, as well as animal and municipal wastes.

In its “Billion-Ton Survey”, Oak Ridge National Laboratory concluded that with relatively modest changes to land use and agricultural and forestry practices, approximately 1.4 billion dry tons of sustainably collected biomass can be collected annually while still maintaining production for food, feed, and export demands (Perlack, et al., 2005). As fossil resources are beginning to show limitations, new attention has been given to this abundant resource. Stepping forward, biorenewable resources have the potential to expand from the conventional uses of building materials, human and food consumption, and direct combustion to provide a variety of higher value products including liquid transportation fuels, replacements for petrochemicals, as well as more efficient ways of providing heat and power, which is the study of this paper.

2.2 Biomass Gasification

2.2.1 Introduction

Gasification is the partial oxidation of solid, carbonaceous fuels into low energy content flammable gas mixtures consisting of carbon monoxide (CO), hydrogen (H_2), nitrogen (N_2), carbon dioxide (CO_2), and a variety of hydrocarbons utilizing high temperatures between 500 to 1400 ℃ and some mixtur e of air, oxygen and/or steam as a fluidizing agent. Gasification is a rather old concept that was commercialized as early as 1812 when coal was converted to “town gas” for use in lighting the streets at night. This technology was spread throughout the industrialized world until a ready supply of natural gas became a cheap alternative in the 1950s. In addition to its history of providing town illumination, gasification has been used as a source of direct fuel and fuel stock during times of energy shortages. During World War II, many people converted their automobiles to run using wood-derived town gas. In times of fuel shortages due to war or embargo, gasification has also served to provide a fuel feedstock for Fischer-Tropsch synthesis of liquid transportation fuels (Brown, 2003).

2.2.2 Reactions

The detailed chemistry of biomass gasification is relatively complex. In the most basic form, biomass gasification can be broken into a two-step process: a pyrolysis step (also known as devolatilization) where the biomass is decomposed by heat into char and volatile materials, and a gasification step where the volatile material and char are converted into the resulting producer gas. The reactions which take place in the gasification step can be classified as exothermic or endothermic based on

whether heat is consumed or produced in the reaction (Ciferno, et al., 2002). The main exothermic and endothermic reactions are summarized in Table 2.1.

Table 2.1 Major reactions occurring in the gasification stage (Ciferno, et al., 2002)

Type of Reaction	Name	Reaction	
Exothermic	Combustion	$C/V + O_2 \rightarrow CO_2$	(1)
	Partial Oxidation	$C/V + O_2 \rightarrow CO$	(2)
	Methanation	$C/V + H_2 \rightarrow CH_4$	(3)
	Water-Gas Shift	$CO + H_2O \rightarrow CO_2 + H_2$	(4)
	CO Methanation	$CO + 3H_2 \rightarrow CH_4 + H_2O$	(5)
Endothermic	Steam-Carbon reaction	$C/V + H_2O \rightarrow CO + H_2$	(6)
	Boudouard reaction	$C/V + CO_2 \rightarrow 2CO$	(7)
	Methane water-reforming	$CH_4 + CO_2 \rightarrow 2H_2 + 2CO$	(8)

*Note: C/V denotes char and volatiles from the biomass

Reactions (1) and (2) are the oxidation reactions and occur in the presence of oxygen from the fluidizing agent. These reactions provide a majority of the excess heat which drives the endothermic reactions (6) and (7). Reactions (3-7) increase the overall concentration of CO and H_2 at high temperatures and in large part determine the resulting composition of the producer gas.

2.2.3 Types of Biomass Gasifiers

The field of gasification has seen various types of gasifiers developed, each having unique benefits and problems associated with their use. At least 15 different gasification technologies are in operation which can generally be classified into three categories by the means of supporting the reactor vessel, fuel and oxidant direction of flow, and method of supplying excess heat to the gasifier (Kirkels, et al., 2011). The first classification, entrained flow gasification, requires finely divided feed material (< 0.1 – 0.4 mm) and was initially developed for coal gasification. This

technique would require a great deal of preprocessing (torrefaction or pyrolysis) before being utilized by biomass (McKendry, 2002). Therefore, this process is not considered in detail in this thesis. The remaining two classifications of gasification reactors are well suited for biomass gasification and include fixed bed and fluidized bed reactors.

2.2.3.1 Fixed Bed Gasifiers

Fixed bed gasifiers can be either updraft or downdraft, denoting whether feedstock moves concurrent or countercurrent to the flow of the gasifying agent. Biomass is fed into the gasifier from the top of the reactor which forms a bed of material which the hot gasification medium moves through. As the material is exposed to temperatures between 750 to 1000 ℃, volatiles are gi ven off from the biomass and ash falls through a grate to the bottom of the reactor.

In an updraft gasifier, also known as a counterflow gasifier, the fluidizing agent is introduced below the grate and diffuses upward through the biomass. Oxidation reactions occur at the bottom of the bed with subsequent reduction reactions occurring higher in the bed. As the hot gases continue up the reactor, the reducing gases (H_2 and CO) pyrolyse the incoming dry biomass, dry the wet biomass, and exit near the top of the reactor. The major disadvantage of updraft gasification is the high tar yield of10 to 20 wt% (Ciferno, et al., 2002).

A downdraft gasifier operates in a very similar manner to updraft except that fuel and gas move in the same direction and the ash and product gas both exit through the bottom of the reactor. Biomass enters through the top of the reactor as high

temperatures drive away moisture from the biomass in a drying step, followed by pyrolysis of the biomass at high temperatures. Next, the gasifying agent is blown into the gasifier and partial oxidation of the char and volatiles generates the required heat for the gasifier. Finally, the volatile and condensable gases are forced through the hot char bed, cracking the tars and increasing product yields of CO and H_2. Downdraft gasifiers result in very low tar yields, but have the disadvantages of more stringent biomass characteristics and limited reactor sizes (Brown, 2003).

2.2.3.2 Fluidized Bed Gasifiers

In a fluidized bed gasifier, a gas stream passes through the reaction bed, created using fine, inert particles, at velocities such that the frictional force between the inert particles and the gas counterbalances the effects of gravity on the particles to form a turbulent mixture of gas and solid. Due to the violent stirring action within the reactor, uniform composition and temperatures between 700 to 850 ℃ exist throughout the fluidized region in such a way that the gasification reactions occur throughout the bed and distinct regions of oxidation, pyrolysis, and reduction do not exist. The two main fluidized bed gasifiers dominant in biomass gasification are bubbling fluidized bed (BFB) and circulating fluidized bed (CFB) reactors (Brown, 2003). The major difference between bubbling and circulating fluidized bed reactors is the velocity at which the fluidizing material enters the reactor vessel. BFB have a velocity right at the minimum fluidizing velocity and thus two zones exist in the gasifier known as the dense phase and the freeboard. Particulate remains in the dense phase, while the freeboard phase allows for the breakdown of tars at the high temperatures (Basu, 2010). CFB reactors have a much higher gas velocity such

that the bed material and char become carried out of the reactor vessel and must be separated via a cyclone and re-injected back into the reactor.

2.2.4 End Use of Gasification Products

Depending on feedstock properties, operating conditions, fluidizing agent and resulting gas characteristics, biomass gasification yields a producer gas capable of a wide variety of applications including heat and power via direct combustion, production of fuels such as hydrogen, methanol, dimethyl ether, gasoline and diesel via catalytic reforming, and production of organic acids, alcohols, and polyesters via syngas fermentation (Brown, 2003). A summary of the desirable producer gas characteristics for the given processes can be found in Table 2.2 at the end of this section.

2.2.4.1 Combined Heat and Power Generation

Air blown gasification results in a low heating value gas which can be used in a combustor to provide process heat and steam for industrial purposes or power generation. This gas can be burned in a gas turbine to provide mechanical work for a generator. In a biomass integrated gasification combined cycle (BIGCC), the hot producer gas is combusted in a gas turbine to generate electricity using a topping cycle while the hot exhaust gas coming from these turbines is used to generate steam to power a steam generator in a bottoming cycle or can provide additional process steam. Overall efficiencies of the BIGCC system have been reported to be as high as 83% with electrical efficiency of 33% (Wang, et al., 2008).

Using producer gas as a fuel for heat and power generation has several key advantages and disadvantages over other uses. Direct combustion for heat only requires that contaminants that will clog downstream processes be removed prior to combustion. Heating values can be low as long as a stable flame can be maintained during the combustion process. Power generation can also utilize low heating value producer gas, although the turbine may have to be derated for the lower valued gas. Additionally, particulates, alkali metals, and tars can deteriorate turbine blades and can clog downstream processes if not properly filtered out (Consonni, et al., 1996).

2.2.4.2 Hydrogen Production

Hydrogen can be used in fuel cells as a “zero emission” transportation fuel. Much effort has gone into the development of hydrogen technologies, yet more research must be conducted in the areas of production, storage, transportation and utilization (Kumar, et al., 2009). Hydrogen has a lower heating value 2.4, 2.8, and 4 times higher than that of methane, gasoline, and coal, respectively, on mass basis and when utilized in a fuel cell can produce up to 60% efficiency. One of the biggest problems facing hydrogen however is the method of production. Approximately 98% of hydrogen is produced by the reforming of fossil fuels, which requires a large energy input and releases harmful GHGs in the process, making the life cycle analysis of hydrogen emissions less promising (Marban, et al., 2007). Gasification of biomass offers an additional method of producing hydrogen from a renewable, clean resource.

In order to increase hydrogen yields, a biomass gasifier may be operated at higher temperatures, higher equivalence ratios, and with the addition of various catalysts within the reactor (Kumar, et al., 2009). Additionally, CH_4 and CO in the producer gas can be reformed using steam to produce additional H_2 using reactions (4), (5), and (8) from Table 2.1.

2.2.4.3 Synthetic Fuels and Chemicals

In order to transform the producer gas into a higher valued product than what can be achieved through combustion, the producer gas may use catalytic processes to upgrade the simple H_2 and CO molecules to larger compounds that are more easily stored and transported. A list of many of the valuable products that can be obtained from a producer gas, and the catalytic pathways by which they are formed can be found in Figure 2.1. In many cases, these reactions must occur under strict temperature and pressure requirements with low levels of impurities and contaminants or the catalysts can be poisoned and the reaction becomes less effective. Significant costs are associated with gas cleanup to prevent impurities from hindering the reactions (Ciferno, et al., 2002).

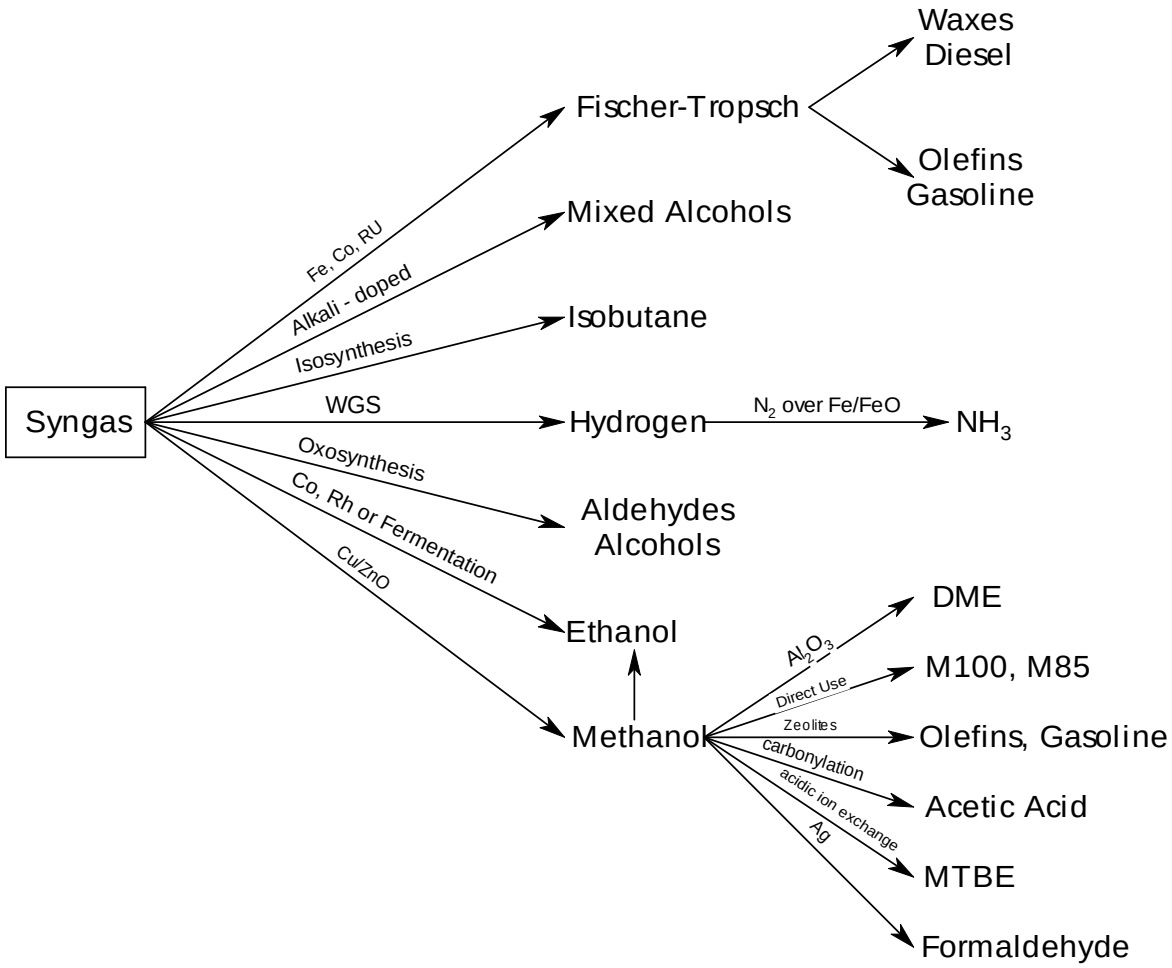

Figure 2.1 Main producer gas conversion pathways (Spath, et al., 2003)

2.2.4.4 Fermentation of Producer Gas to Ethanol

The fermentation of producer gas to ethanol combines both thermochemical and biochemical pathways for the production of fuel from biomass. This process is attractive due to the selectiveness of the micro-organisms which convert the H_2 and CO into ethanol. In comparison to traditional methods of fermenting biomass to ethanol, fermentation of producer gas allows for a much wider selection of biomass

resources. Equations (9) and (10) below list the conversion process completed by the micro-organisms during the fermentation process (Kumar, et al., 2009).

$$6CO + 3H_2O \rightarrow C_2H_5OH + 4CO_2 \quad (9)$$

$$6H_2 + 2CO_2 \rightarrow C_2H_5OH + 3H_2O \quad (10)$$

The field of microbiology is constantly working to identify and engineer new microorganisms capable of converting various inputs to a wide variety of other products as well including organic acids, alcohols, and polyesters.

Table 2.2 Desirable producer gas characteristics for various applications (Ciferno, et al., 2002)

Product	**FT Gasoline and Diesel**	**Methanol**	**Hydrogen**	**Fuel Gas**	
				Boiler	Turbine
H_2/CO	0.6	~2.0	High	Unimportant	Unimportant
CO_2	Low	Low	Unimportant	Not Critical	Not Critical
HCs	Low	Low	Low	High	High
N_2	Low	Low	Low	Unimportant	Unimportant
H_2O	Low	Low	High	Low	Not Critical
Contaminants	< 1 ppm Sulfur Low Partic.	< 1 ppm Sulfur Low Partic.	< 1 ppm Sulfur Low Partic.	Small amounts tollerated	Low Partic. & Metals
Heating Value	Unimportant	Unimportant	Unimportant	High	High
Pressure (bar)	~20-30	~50 (vapor) ~140 (liquid)	~28	Low	~400
Temperature (℃)	200-400	100-200	100-200	250	500-600

2.3 Effect of Biomass Feedstock on Producer Gas Composition

One of the main advantages of biomass gasification is the ability to use a wide range of feedstocks with relatively small changes to the setup and operation of the gasifier. This allows for a more abundant supply of feedstock compared to other means of biofuel production that are limited to a small selection of biomass sources. In spite of this obvious advantage, differences in the composition of various feedstocks, as well as the feedstock properties can vary the composition of the resulting producer gas. The non-homogeneity of various feedstocks pose difficulties in maintaining constant feed rates to the gasification unit as well as ensuring a consistent producer gas composition.

Feedstock properties that have the greatest impact on the performance of the gasifier and overall producer gas composition include moisture content, ash content, volatile compounds and particle sizes. Fuel with moisture contents above 30% make it difficult to maintain bed temperatures due to the need to drive off excess moisture before pyrolysis and combustion can occur, resulting in uncracked hydrocarbons released in the pyrolysis zone. Additionally, excess moisture in the presence of CO will lead to increases of H_2 and CH_4 by means of the water-gas shift and hydrogenation reactions. Heating values of the final producer gas compositions are typically lower when too much moisture is present. High levels of ash in a biomass, especially ash with high alkali oxides and salts, often have lower melting temperatures than the overall oxidation temperature and can result in slagging problems in the reactor. Biomass contains very high levels of volatile content (70-90 wt%) which is released during the pyrolysis stage and is reacted with the char to

produce H_2 and CO. Higher levels of volatile content in the biomass will result in a higher yielding producer gas. Finally, the particle size of biomass can affect the overall producer gas composition. If particles are too large, bridges can form in the gasifier which prevent continued flow in the gasifier but if particles are too small, natural voids created in the reactor bed become clogged and the gasifying agent is not allowed to pass through the reactor. Both scenarios yield poor reactor performance (McKendry, 2002).

Lignocellulosic biomass is composed of three main constituents including cellulose, hemicellulose and lignin. Herbaceous crops and wood contain 60 to 80% cellulose and hemicellulose and 10 to 25% lignin on a dry basis. The carbon conversion efficiencies are 97.9%, 92.2% and 52.8% for cellulose, hemicellulose, and lignin, respectively. Concentrations of each of these components will affect the overall producer gas composition. For example, at 900 ℃, cel lulose resulted in 35 mol% CO, 6 mol% CH_4, 26 mol% CO_2 and 29 mol% H_2 while hemicellulose and lignin resulted in 25 mol%, 5 mol%, 36 mol% and 33 mol% respectively (Kumar, et al., 2009).

Another important observation about the effect of feedstock on producer gas composition is that the nitrogen content in biomass is directly related to the amount of ammonia in the producer gas (Yu, et al., 2007). This phenomenon is of great interest to this study and will be developed further in Section 2.4 of this review.

2.4 Fate of Nitrogen in Biomass Feedstock

Nitrogen is a nutrient required by plants for the formation of amino acids and proteins necessary for their growth and is absorbed by the root of plants as NO_3^- and NH_4^+. These compounds must move from the root of the plant through the xylem and into the young leaves and stems where growth is occurring. Here, the compounds are converted to proteins and amino acids. Thus, a majority of the nitrogen found in biomass exists in the leaves and stems of the plant (Zhou, et al., 2000). During gasification, the fuel bound nitrogen (FBN) is first released in the form of tars. Upon passing through the high temperature char, the tars are cracked and part of the nitrogen contained within is released as ammonia, hydrogen cyanide, molecular nitrogen, and various oxides of nitrogen (Mandl, et al., 2011). The resulting concentration of nitrogen compounds depends on the biomass properties and gasification operating conditions. Numerous studies have shown the primary nitrogen bearing compounds in biomass gasification to be ammonia (NH_3) and hydrogen cyanide (HCN), with NH_3 being the predominant compound formed. Table 2.3 shows the results of various studies on producer gas nitrogen composition for various feedstocks. The oxidation of these species at high combustion temperatures readily produces high NO_x emissions. Under oxygen starved conditions, the same nitrogen bearing precursors can be reduced to N_2 and is often used as a NO_x control strategy (Whitty, et al., 2010)

Table 2.3 Producer gas nitrogen distribution for various feedstocks

Raw Material	Reed Canary Grass[a]	Miscanthus[a]	Salix[a]	Leucaena[b]
% of fuel N in char	0.7	9.4	0.0	2.0
% of fuel N as NH_3	34.3	12.7	24.4	13.49
% of fuel N as HCN	0.10	0.12	0.22	0.07
% of fuel N as NO	0.20	0.04	0.66	0.02
% of fuel N as NHC	1.30	0.37	0.67	-
Ratio (%) of N(HCN) to N(NH_3)	0.29	0.94	0.90	-
Ratio (%) of N(NO) to N(NH_3)	0.58	0.31	2.70	-

[a] Fluidized bed gasifier operated 900 ℃, 0.4 bar (Yu, et al., 2007)

[b] Fluidized bed gasifier operated at 900 ℃ , ~atmospheric pressure (Zhou, et al., 2000)

2.4.1 NOx Formation Pathways during Combustion

NO_x is a term used to describe the various oxides of nitrogen that are important in combustion and emission studies. The three primary compounds are nitric oxide (NO), nitrogen dioxide (NO_2) and nitrous oxide (N_2O). Nitric oxide is the primary emitted species of the NO_x constituents and is typically of primary concern when studying combustion emission. Although at the levels present in the environment, NO causes minimal health or environmental problems, it can be oxidized to NO_2 which is generally considered more harmful. NO_2 can be oxidized further in the atmosphere to produce ozone, or can contribute to photochemical smog and acid rain when it is reacted with OH to form HNO_3. N_2O is generally a minor constituent of total NO_x yet is still of great importance as it has a global warming potential 298 times greater than carbon dioxide (Whitty, et al., 2010). NO_x can be formed through three different mechanisms, while two of them dominate combustion of syngas. Figure 2.2 shows a simplified schematic of the NO_x pathways and a brief discussion of each mechanism follows.

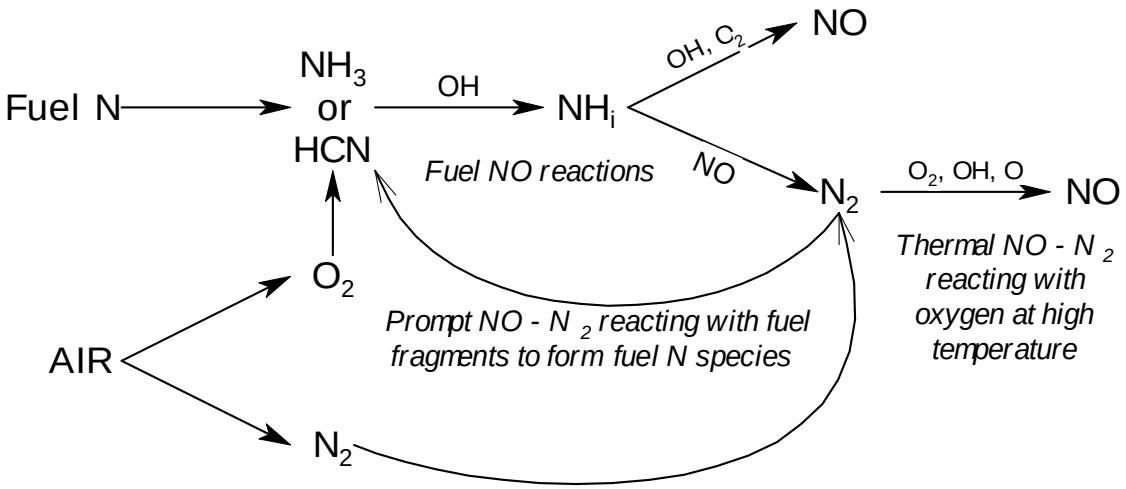

Figure 2.2 Main NO_x production mechanisms (Whitty, et al., 2010)

2.4.1.1 Prompt NO_x

Prompt NO_x is the formation of NO very rapidly in the flame zone due to the presence of hydrocarbon fragments (i.e. HC) and NNH radicals. Due to the rapid creation of the NO molecules over a very short time scale, contribution to overall NO_x by the prompt NO_x mechanism is small, and is generally neglected in combustion emission studies (Turns, 2000).

2.4.1.2 Thermal NO_x

Thermal NO_x results from the oxidation of molecular nitrogen (N_2) from the incoming combustion air at high temperatures. The fundamental reactions for this process are given by the extended Zeldovich mechanism as follows (Whitty, et al., 2010):

$$O + N_2 \leftrightarrow NO + N \quad (11)$$

$$N + O_2 \leftrightarrow NO + O \quad (12)$$

$$N + OH \leftrightarrow NO + H \quad (13)$$

Due to the relatively large activation energies associated with the reactions in the extended Zeldovich mechanism, the thermal NO_x mechanism has a very strong temperature dependence. As a result, thermal NO_x is usually unimportant at temperatures below 1800 K (Turns, 2000).

2.4.1.3 Fuel NO_x

Fuel NO_x occurs when nitrogen containing species within the producer gas are oxidized at high temperatures to form either NO or N_2 depending on the local combustion conditions. The two major nitrogen precursors found in biomass-derived producer gas are NH_3 and HCN, with ammonia being the dominant species concentration. Several lab scale studies have investigated the effect of NH_3 in various synthesis gas flames. It is showed that the specific NO_x precursor is less important in determining overall NOx levels when compared the importance of fuel-N dopant level and the flame configuration (Sarofim, et al., 1978). From the combustion of a laminar coflowing, nonpremixed methane air flame seeded with various amounts of NH_3, it was also found that while greater seeding of NH_3 resulted in increased NO_x emissions, increased levels of NH_3 also yielded a higher percentage being converted to N_2 rather than NO_x (Sullivan, et al., 2002). Details of the ammonia oxidation method are shown in Figure 2.3.

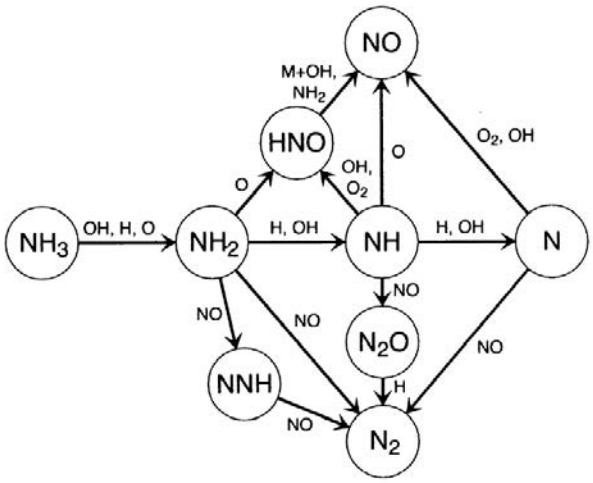

Figure 2.3 NH_3 oxidation mechanisms, reproduced from (Sullivan, et al., 2002)

2.5 Producer Gas Combustion

2.5.1 Fundamental Considerations in Producer Gas Combustion

Apart from the adiabatic flame temperature, the laminar flame speed, ignition temperature and delay, and flame extinction limits are the most important properties to be considered in the analysis of the combustion properties of any gas. Due to the complexity introduced when investigating both the major and minor components in the producer gas, many studies have investigated the combustion properties of only the major species in producer gas, carbon monoxide (CO) and hydrogen (H_2). The ignition and flame propagation characteristics of various CO/H_2 mixtures were studied under pressures ranging from 1 to 40 atm. The study shows for a wide variety of pressure conditions that the flame speed increases at higher concentrations of H_2 in a H_2/CO mixture (Sung, et al., 2008). Ribert, et al. (2010) reported similar findings for various CO/H_2 mixtures at atmospheric pressure and equivalence ratios spanning the flammability limits of $\varphi = 0.35$ and $\varphi = 5$. The results of this study are presented in Figure 2.4.

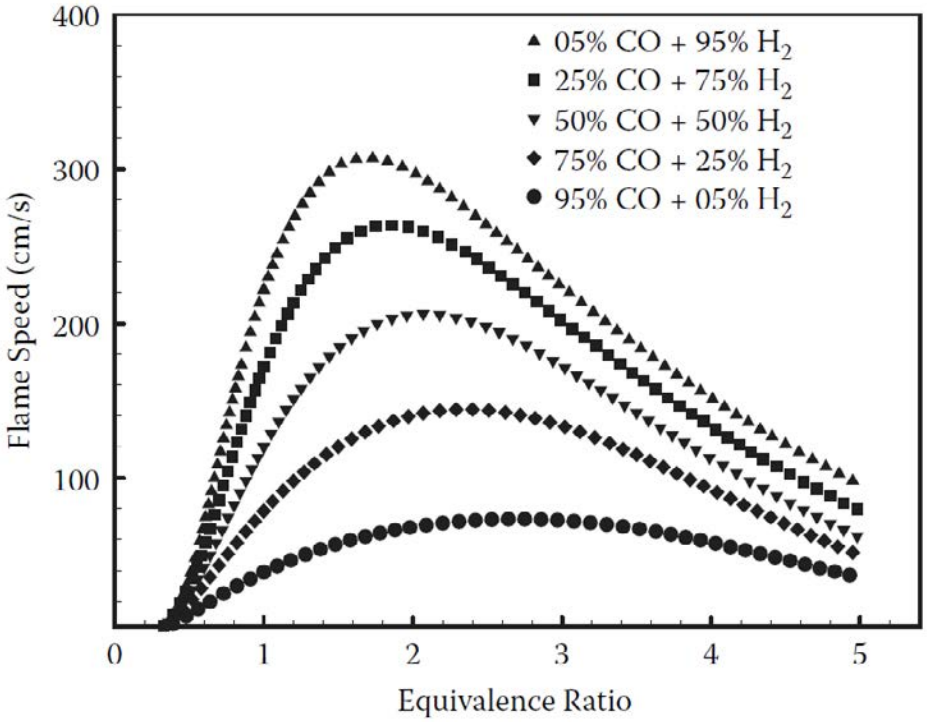

Figure 2.4 Laminar flame speeds of H_2/CO mixtures at p = 1atm and T_{in}=300K Reproduced from (Ribert, et al., 2010)

Fotache, et al. (2000) investigated the ignition characteristics of counterflowing CO/H_2 vs. heated air gas mixtures and found the existence of three ignition regimes that are a function of hydrogen concentration in the flame. It is found for concentrations of H_2 below 7%, the ignition temperature is strongly dependent on hydrogen concentration. For concentrations in excess of 17 to 20% H_2, ignition temperatures seem fairly constant. The third ignition regime is from 7-17% which is a transition stage, and is the intermediate between the first two regimes (Fotache, et al., 2000).

Finally, and perhaps most relevant to this thesis research, a study investigating the combustion of CO/H_2/CH_4 in premixed flames was conducted to examine blowout, flashback, autoignition and stability properties of various fuel gas compositions and it

is found that the behavior of fuel mixtures can be drastically different than that of the individual constituents (Lieuwen, et al., 2008). In particular, the significantly different transport properties and flame speed of hydrogen provides many unique interactions when mixed in these fuels. Additional study on the effects of fuel composition to the various properties of the fuels is highly recommended (Lieuwen, et al., 2008).

2.5.2 Low-Swirl Burner

An analysis of the combustion properties of a gas requires very simple flames that are easy to characterize. The application of these gases, however, requires a much more complex flame in order to improve overall combustion. Swirling flow burners have been used extensively in both premixed and non-premixed lean combustion systems to increase flame stability, combustion intensity and combustor performance. Swirl burners utilized in gas turbines and industrial furnaces create powerful vortexes within the flame that increase the speed of collision between axial and tangential flows, speeding up the mixing time for air and fuel, and extending the residence time. In a low-swirl burner, swirling air and fuel exit into a furnace or the atmosphere at swirl numbers between 0.4 and 0.55 (Surjosatyo, et al., 2011). The use of low-swirl burners is a rather new concept in the combustion of producer gas, and studies are just beginning to emerge in literature.

Zhou, et al (2002) used small amounts of ammonia added to a methane/air fuel for turbulent combustion in order to study the relationship between turbulence and chemistry in NO formation. In particular, the effect of swirl number was investigated for various methane/air/ammonia flames. Results showed several interesting trends.

First, increasing swirl numbers will lead to first an increase and then a decrease in combustion temperature at the exit, corresponding to an increase in thermal NO_x followed by a decrease. At the same time, the increase of swirl number will first cause a decrease and then an increase of fuel NO due to greater turbulence in the flame (opposite to the trend for thermal NO_x) (Zhou, et al., 2002).

Adouane, et al. (2003) used natural gas with very small amounts of ammonia (1300-2000 ppm) in the preliminary development of a low NO_x combustor for biomass derived gas in a dual-stage, high-swirl, lean combustor. Results for NO_x emissions as a function of equivalence ratio show the greatest reduction in NO_x emissions occurs at slightly fuel-lean conditions of around 4% excess oxygen. The trend follows a gradual decline in NO_x emissions from 0% to 4% excess oxygen, followed by a much steeper rise thereafter (Adouane, et al., 2003).

Bhoi, et al. (2009) investigated the combustion of babul wood derived producer gas in a low swirl, premixed gas burner that allowed for the modification of various burner parameters including swirl angle and bluff body diameters. This study investigated the effect of swirl angle on temperature and emissions over a range of flow rates. It was found that an optimal swirl angle of 60° produced nearly the highest maximum mean flame temperature and optimal NO_x reductions. Additionally, it was found that NO_x emissions decrease with increasing swirl angle and that CO emissions are independent of swirl angle for A/F ratios of 1.0, or 3 to 4.5% excess air (Bhoi, et al., 2009). In a preceding study of this same combustion system attempting to optimize the combustion system, it was found that NO_x

emissions tended to be independent of thermal input while CO and UHC emissions decreased with increasing thermal input (Bhoi, et al., 2008).

Another study of babul wood derived producer gas studied the effect of A/F ratio on flame temperature and various emissions in a premixed low-swirl burner. It was found that highest temperatures are achieved with A/F ratio around 1.0. NO_x and CO emissions were investigated for A/F ratios from 0.8 to 1.5 and was found that NO_x emissions peaked with and A/F ratio of around 1 and decreased at higher and lower A/F ratios. CO remained constant for A/F ratios of 0.8 to 1.25 and then increased at A/F ratios higher than 1.25 for all flow rates investigated (Panwar, et al., 2011).

Finally, and investigation of low-swirl premixed injectors for implementation in gas turbines in the integrated gasification combined cycle power plants was investigated. This study investigated various compositions of $CO/H_2/CH_4$ in low swirl injectors and found that these injectors were capable of burning up to 60% H_2, and that gases with high H_2 concentrations had lower lean blow-off limits. Additionally, NO_x emissions are reported to show a log-linear dependency on the adiabatic flame temperature of the gas (Littlejohn, et al., 2010).

From the above literature review, it is obvious that general understanding of natural gas and producer gas combustion, especially in low swirl burners, is still lacking. Thus, further investigations in to the combustion of producer gases derived from different feedstocks, and the importance of fuel bound nitrogen combustion and emissions in such environments should be further investigated.

2.6 Biomass Gasification Modeling

As competition for funding and limited resources continues to rise in an economy that is dominated by fearful investors, the use of accurate models to simulate various systems and designs before making an investment is becoming increasingly more important. The details of gasification kinetics are very complex and currently are not well understood for a wide variety of feedstocks. Therefore, several types of gasification models have emerged, each with advantages and disadvantages. The kinetic rate models that do exist are computationally quite intensive, yet can give accurate and detailed results. The limitation of the kinetic models lies in the feedstock specific parameters contained within the model, limiting the applicability to study different biomass feedstocks. Thermodynamic equilibrium models are independent of gasifier design and feedstock inputs, and thus may be more beneficial for the study of macro-scale fuel process parameters. These models make several broad assumptions about the overall gasification process and can often introduce significant differences in predictions when compared side-by-side. An excellent review of the current kinetic and thermodynamic modeling efforts is available and further inquiry should be directed to this article (Puig-Arnavat, et al., 2010).

Aspen Plus gasification models provide some of the simplest models available that incorporate the principle gasification reactions and the overall physical characteristics of the gasification reactor. This system is a problem-oriented program that is used to calculate physical, chemical, and biological processes using many separate modules, which can be tested independently, to produce the whole.

A comprehensive gasification model was developed with external FORTRAN subroutines to model a lab-scale pine gasifier with good agreement with experimental results for pine wood (Nikoo, et al., 2008). Hannula, et al. (2010) developed a model containing eight main blocks with FORTRAN subroutines for various chemical conversions and found his model to closely simulate pine sawdust, pine and eucalyptus chips, and forest residues, but could not simulate pine bark or wheat straw (Hannula, et al., 2010). Other studies also explore various gasification models that are applicable only to a single set of data and limited feedstocks (Doherty, et al., 2008), (Tan, et al., 2010), (Proll, et al., 2008).

As can be seen by the above literature review, numerous Aspen Plus models have been created to simulate the gasification of biomass yet the vast potential for various feedstocks and differences in operating conditions signifies that models must be developed and customized to feedstock and technology specific requirements in order to obtain the most accuracy. The modeling section of this work will attempt to produce an Aspen Plus model capable of simulating a pilot-scale gasification system utilizing wood as a feedstock.

CHAPTER 3. GASIFICATION MODEL

3.1 Introduction

This chapter summarizes the gasification and combustion system from which the experimental data are taken for the present model as well as the modeling techniques used to carry out this study. This study is based on a pilot-scale gasification system at the Bio-energy conversion (BECON) facility, administered by Iowa Energy Center. The original experiments were designed to study the effect of feedstock on producer gas composition. In particular, various feedstocks with controlled nitrogen content were gasified under the same operating conditions. Data were collected for overall producer gas composition as well as for emissions from combustion when burned in an industrial burner. The following section only provides a brief description of the system since this work is focused on modeling. A more detailed description of the system, data collection techniques, and results can be found in a previous study (Sethuraman, et al., 2011).

3.2 Description of Gasification and Combustion System

Data were collected from a 180 kg/hr biomass fed, fluidized bed reactor, pilot-scale gasification system. This system consists of a screw-drive feed auger, a pressurized vessel, a fluidized bed reactor, and baghouse-type gas cleaning components as shown in Figure 3.1. When the equivalence ratio is defined as the ratio of the actual air-fuel ratio to the stoichiometric air-fuel ratio, the gasifier is operated under an equivalence ratio between 0.22 and 0.25 (i.e., fuel rich operation). This definition is common to the gasification industry, but is the inverse of traditional combustion theory.

Figure 3.1 Bubbling fluidized bed gasifier

Dry, pelletized biomass is delivered to the BECON facility ready for input to the gasification system. The biomass is first loaded into the feeding auger which limits the size of pellet that can be gasified to a diameter of one inch. The pellets that were used in this experiment were approximately 15 mm in length and 5mm in diameter. The feed auger delivers the biomass at a constant rate to a vessel, which is pressurized to 15 to18 psi once full of biomass. Once pressurized, the biomass passes into a second pressurized vessel kept at the same pressure as the first. From this point, the biomass is finally introduced to the bubbling fluidized bed reactor. This reactor, operated at atmospheric pressures, receives fluidizing air from

the bottom of the reactor and has a bed depth of 1 to 1.3 meters. The temperature inside of the reactor is maintained at 815 ℃ using el ectric heating coils and is monitored using four K-type thermocouples.

When the biomass is exposed to the high temperature, low oxygen conditions present in the gasifier, the biomass begins to break down and results in a producer gas consisting of hydrogen, carbon monoxide, nitrogen, methane, and various other hydrocarbons, ammonia, water, tar, and char. Producer gas compositions for various feedstocks are listed in Table 3.1. This producer gas leaves the gasifier at bed temperatures and a pressure ranging from 15-18 psig. In order to prevent clogging of downstream components, heavy ash and char particles must be removed from the producer gas through the use of a baghouse filtration system. The baghouse is essentially a cyclone filter, which separates heavy char and ash particles by gravimetric methods. Due to design constraints, gas temperatures must not exceed 400℃ in the baghouse, yet must be kept above the tar condensation temperature of 316 ℃. Therefore, after exiting the fluidized bed reactor, the producer gas passes through a heat exchanger which cools the gas below 400 ℃ and electric heating coils inside the bagh ouse maintain gas temperatures above 316 ℃. Gas exiting the baghouse is usually at 5 psig and 350 ℃.

Table 3.1 Producer gas compositions for various feedstock (Sethuraman, et al., 2011)

Feedstock	Wood	Wood+20 % DDGS	Wood+40 % DDGS	Wood+70 % DDGS
% Nitrogen In Biomass	0.14	0.95	1.75	2.81
Components of Producer gas				
Nitrogen (N_2)	39.02	39.86	41.51	50.57
Carbon monoxide(CO)	16.91	15.86	12.55	12.54
Hydrogen (H_2)	11.33	8.97	7.01	4.39
Carbon dioxide (CO_2)	13.56	14.01	12.87	10.98
Methane (CH_4)	5.27	5.68	5.17	4.50
Ethane (C_2H_6)	0.26	0.25	0.29	0.43
Ethylene (C_2H_4)	1.18	1.83	1.93	2.36
Acetylene (C_2H_2)	0.07	0.12	0.10	0.15
Propane (C_3H_8)	0.07	0.10	0.17	0.18
Ammonia (NH3)	0.06	0.23	0.24	1.15
Water (H2O)	9.97	13.58	18.63	12.33
Lower heating value (MJ/kg)	5.58	5.52	4.96	4.83
Adiabatic flame temperature (K)	1932	1908	1822	1825

A medium velocity, industrial burner rated for a maximum input of 879 kW was used for producer gas combustion. The producer gas exiting the baghouse passes through an orifice plate flow meter to measure the flowrate before entering the non-premixed burner at temperatures of around 325 ℃. A combustion chamber built with refractory lining surrounds the burner in order to prevent heat loss, limit environmental variables, and carry away exhaust gases. The combustion chamber is shown in Figure 3.2. Atmospheric air passes through a thermal gas mass flow meter and is blown by a motor into the combustion chamber, entering the chamber in four different stages allowing for staged combustion. The first three stages limit the amount of air entering the burner creating fuel rich combustion. The final stage creates a fuel lean zone where any remaining hydrocarbons are consumed.

Average flame length is around 1 m but varies according to feedstock characteristics and the equivalence ratio of combustion. Thermocouples are placed at various heights on the axis throughout the combustion chamber to monitor temperature distribution in the chamber and to ensure overall temperatures did not exceed the maximum design temperature of 1316 ℃. A schematic of the overall gasification and combustion system is shown in Figure 3.3.

Figure 3.2 Combustion chamber

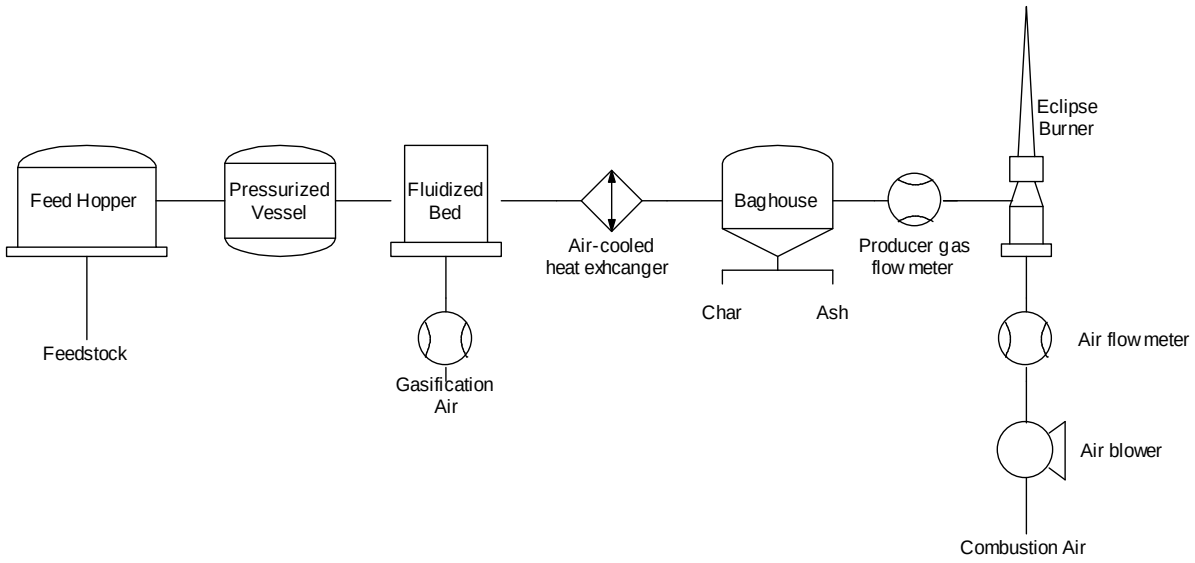

Figure 3.3 Schematic representation of the present gasification and combustion system

In addition to the gasification and combustion capabilities discussed above, the BECON facility provides means for the accurate recording of temperature and flow information throughout the system as well as composition analysis for both the producer gas and the exhaust gases. This information was implemented into an Aspen Plus model as discussed in the next section.

3.3 Description of Aspen Plus Model

The BECON gasifier is modeled as a 180 kg/hr pine wood-fed gasification system that produces a low to mid-grade producer gas to be used for process heat or power generation. This system utilizes an atmospheric, air blown fluidized bed reactor. The main processes modeled include: gasification (A100) where the biomass is subject to high temperatures in a low oxygen environment, producer gas cleaning (A200) where the heavy char and ash particles are removed, and gas combustion

(A300) where the producer gas is combusted to produce heat. The breakdown of the various process areas is shown in Figure 3.4.

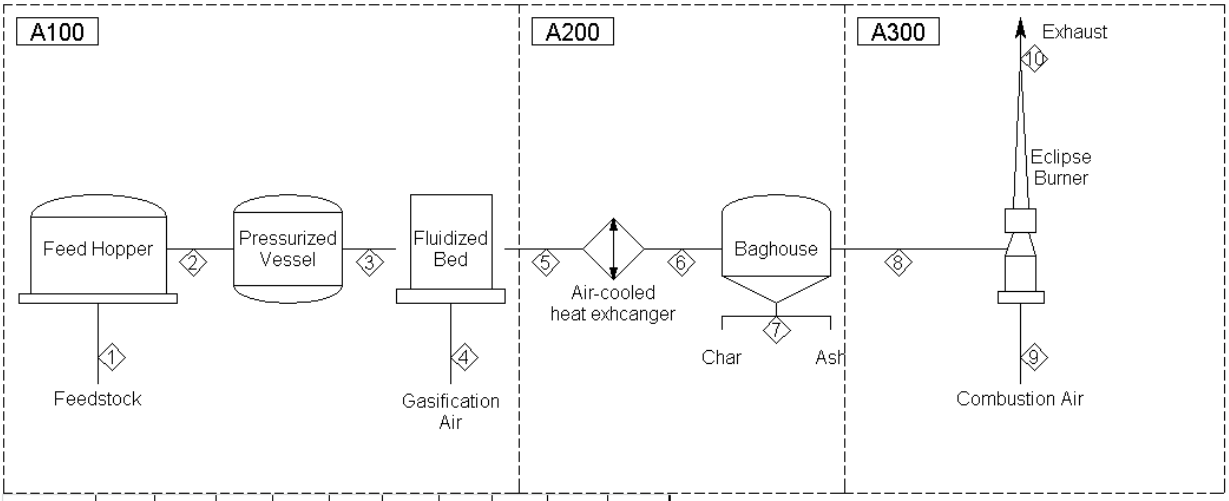

Stream	1	2	3	4	5	6	7	8	9	10
T (°C)	25	25	25	25	815	350	350	350	25	1500
P (bar)	1.01	1.01	1.24	1.24	2.25	2.05	2.05	2.05	1.01	1.01
m (Mg/day)	4.32	4.32	4.32	4.63	8.95	8.95	0.29	8.65	17.93	26.59

Figure 3.4 Overall process diagram (parallelograms enclosing numbers in the diagram designate individual process streams)

3.3.1 Area 100 Gasification

The gasification area (i.e., submodel) contains the feed hopper, pressurizing vessel, as well as the fluidized bed gasifier. Feedstock enters the biorefinery at 6 wt% moisture level. Pine wood elemental composition is shown in Table 3.1. Ash content is assumed to be 6 wt%. Char composition, as formed in the gasifier, is also shown in table 3.1.

Table 3.2 Pine wood and char elemental compositions (wt%)

Element	Wood	Char
Ash	6.00	0
Carbon	46.56	63.05
Hydrogen	6.24	0.71
Nitrogen	0.14	0.29
Chlorine	0	0
Sulfur	0.02	0.04
Oxygen	46.13	35.91

The gasification model uses a set mass ratio of oxygen to biomass based on the gasification temperature of 815 ℃. A mass ratio baseli ne value of 0.26 was developed in a previous study in which woody biomass was gasified under similar temperature conditions to the current case (Bain, 1992). This ratio was then adjusted until appropriate producer gas yields were obtained from the model. Equilibrium conditions are very difficult to model at such low temperatures, so an elemental balance calculation and adjustment is preformed to insure complete mass balance across the gasifier. Details on this calculation can be found in Appendix B.

3.3.2 Area 200 Gas Cleanup

The BECON gasification plant implements most basic methods of gas cleanup. The choice of utilizing the producer gas for direct combustion reduces the requirement for cleanup that must occur by only needing to remove heavy particulate matter to prevent downstream clogging. Before the hot producer gas can be cleaned, a heat exchanger cools the gas from the inlet temperature of 815 ℃ to a temperature of 350 ℃. After being cooled to safe temperatures, the baghouse is utilized to remove both char and ash content from the producer gas before it is sent to the combustor.

A baghouse is essentially a cyclone filter and as such, is modeled as a system of two cyclones in series which remove 99% of particulate matter. The first cyclone is a medium efficiency unit which removes 88% of the particulate matter while the second cyclone is a high efficiency unit which will finish removing the particulate to 99% removal efficiency.

3.3.3 Area 300 Producer Gas Combustion

After removing the particulate matter in the gas cleanup section, the producer gas enters the combustion area of the model where it is burned equivalence ratios between 1.15 and 2.0, where equivalence ratio is defined as actual air fuel ratio divided by stoichiometric air-fuel ratio. The combustor is assumed to operate adiabatically resulting in an exit flue gas temperature of approximately 1900 ℃. Air flow rate into the combustor is calculated by determining the stoichiometric amount of oxygen required and multiplying it by the amount of excess oxygen desired for the set equivalence ratio.

CHAPTER 4. EXPERIMENTAL SETUP

4.1 Introduction

This chapter summarizes the combustion system and the measurement method used to carry out this study. Each section outlines the capacities of the different components, limitations of different techniques and methods used to conduct the experiments.

4.2 Vertical Updraft Swirl Combustion Rig

A lab-scale Vertical Updraft Swirl (VUS) Combustion system was used to conduct the experiments. Figure 4.1 shows the setup for the VUS combustor. Air enters through a 1” NPT fitting into the bottom plate of a 12” - diameter by 10” - tall air plenum to distribute the air and ensure even flow through the air swirler exit, which is mounted to the top plate of this plenum. On the side of the air plenum are two 3/8” Swagelok male adapters from which syngas can be piped directly to the inner and outer ports of the gas injector. Mounted to the top plate of the air plenum is a two-foot long, 120 mm - diameter Pyrex tube which houses the flame during combustion, and provides optical access to view the combustion process. An aluminum cap mounted above the glass combustion chamber is held in place by two rods of 3/8” all-thread, providing both rigidity and structure to the VUS combustor. An exhaust gas sample line and a thermocouple enter the flame through the aluminum cap and sample the exhaust gas from 23 inches above the injector. This sample is then sent through the exhaust measurement system (described in Section 4.4) for analysis.

Figure 4.1 VUS combustion rig

Figure 4.2 shows a cutaway diagram of the two-piece prototype injector and swirler components used in this experiment that were designed by Goodrich Corporation at the West Des Moines, IA location. The stainless steel injector allows for the injection of two separate gas streams through two ports that are supplied from the Syngas

Delivery System (described in Sec 4.3). The inner-port is a straight tube injection, allowing flow rates between 0-10 standard liters per minute (SLPM), although the higher flow rates can lead to higher incidence of flame blowout. The outer-port imparts a slight swirl to the gas as it leaves the injector and is capable of running flow rates of gasses at much higher rates, up to the order of 100 SLPM. For the purposes of this experiment, only the outer injection port was used to supply the syngas at approximately 21 SLPM because of its ability to support higher flow rates.

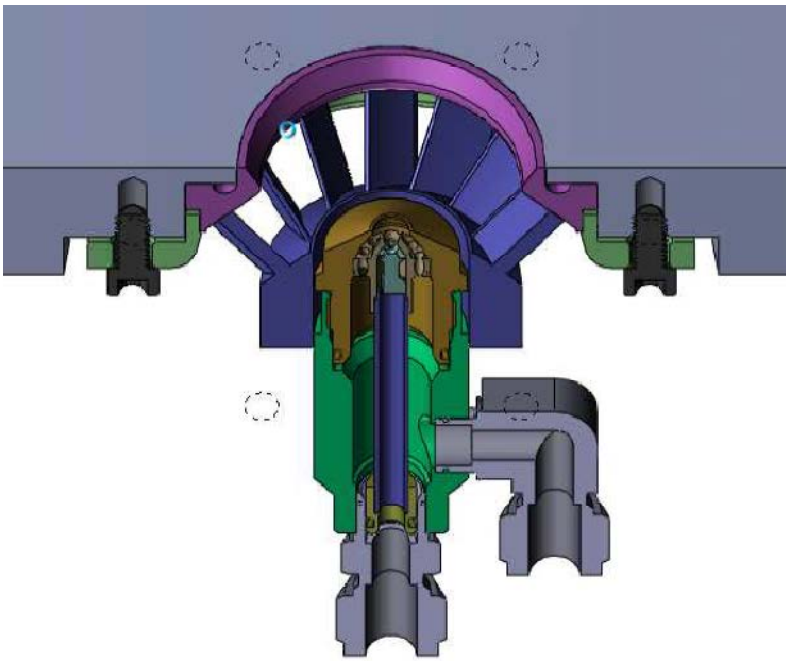

Figure 4.2 Injector and swirler diagram

Goodrich supplied four swirlers which mate to this injector with varying effective flow areas as summarized in Table 4.1. These swirlers were fabricated by Goodrich using a nanoceramic resin on a rapid prototype machine and are rated for 600℉ temperatures, but have been shown to withstand temperatures of up to 900℉, when

the flame is not attached. In order to see the highest resolution of NOx in the final measurements, swirler 1, which has an effective area of 2.00 in^2, was chosen. The spark ignition for the VUS combustor is supplied from a 120 volt AC power source which converts the signal to 20kV at 35 mA Peak. Two lead wires pass through the air plenum into the combustion chamber where they spark directly above the gas injector.

Table 4.1 Swirler effective areas

No.	Effective Area	Swirl Strength
1	2.00 in^2	Weakest
2	1.87 in^2	
3	1.66 in^2	
4	1.52 in^2	Strongest

The VUS combustor is limited by a number of constraints. The maximum temperature which can be sustained by the pyrex glassware is 914℉. Additionally the swirler composite material is also constrained by a similar temperature. This limits the total flow rate that can be combusted in the VUS combustor and also limits the combustor to lab scale tests.

4.3 Producer Gas Delivery System

In order to study a wide variety of gas mixtures, a nine-unit Alicat Mass Flow Controller (MFC) system was used, as shown in Figure 4.3. The Alicat MFCs operate by determining the volumetric flow rate of the gas by creating a pressure drop across a Laminar Flow Element (LFE) and measuring the differential pressure across it. Poiseuille's equation is then used to calculate the flow rate of the selected gas. For accurate measurements to be taken, the correct gas must be selected so that the appropriate gas viscosity can be used by the MFC to calculate the flow rate.

Once the desired flow rate is input to the MFC, a valve is actuated to achieve the desired flow rate. The MFC flow rates ranged from 200 SCCM (standard cubic centimeters per minute) to 1500 SLPM (standard liters per minute) and were capable of supporting more than 30 different non-corrosive gases. Additionally, two of the MFCs were manufactured to support corrosive/aggressive gases, allowing for accurate control of ammonia into the syngas mixture. One MFC was further customized to accurately control the final 10-component syngas used in the final stage of this experiment. All nine MFCs were connected to an Alicat BB9 communications module, and were linked via serial cable to a computer which used a Labview program to control the units.

Figure 4.3 Mass flow controller setup

The Mass Flow Controller system was supplied with various gases from three separate locations, allowing for the isolation of flammable gases from oxidizers as well as vented storage for all noxious gases including ammonia and carbon monoxide. The vented gases were stored in a separate room and were piped through the concrete wall and supplied to the MFCs as appropriate as shown in Figure 4.4. After passing through the MFCs, the various gases were mixed in a gas manifold and were then sent to the combustor via 3/8” polyethylene tubing. Compressed air was supplied via a ½ inch in-house air line at 90 psi and was sent to the VUS combustor’s air plenum via a 1” reinforced rubber hose.

Figure 4.4 Vented gas supply

A Labview program was developed to control the array of MFCs from a single computer system using RS-232 serial binary control commands. Using this system, each mass flow controller must be manually configured to have a unique UnitID ranging from A to I, and must be set to what gas is being used. After this manual setup on each MFC, the Labview program can send new set-points to each MFC, and can read temperature, pressure, as well as mass and volumetric flow rates from each MFC. Additionally, a STOP button is programmed to give a zero set-point to

each MFC before shutting down the program in case of emergency. A screenshot of the Labview interface is shown in Figure 4.5.

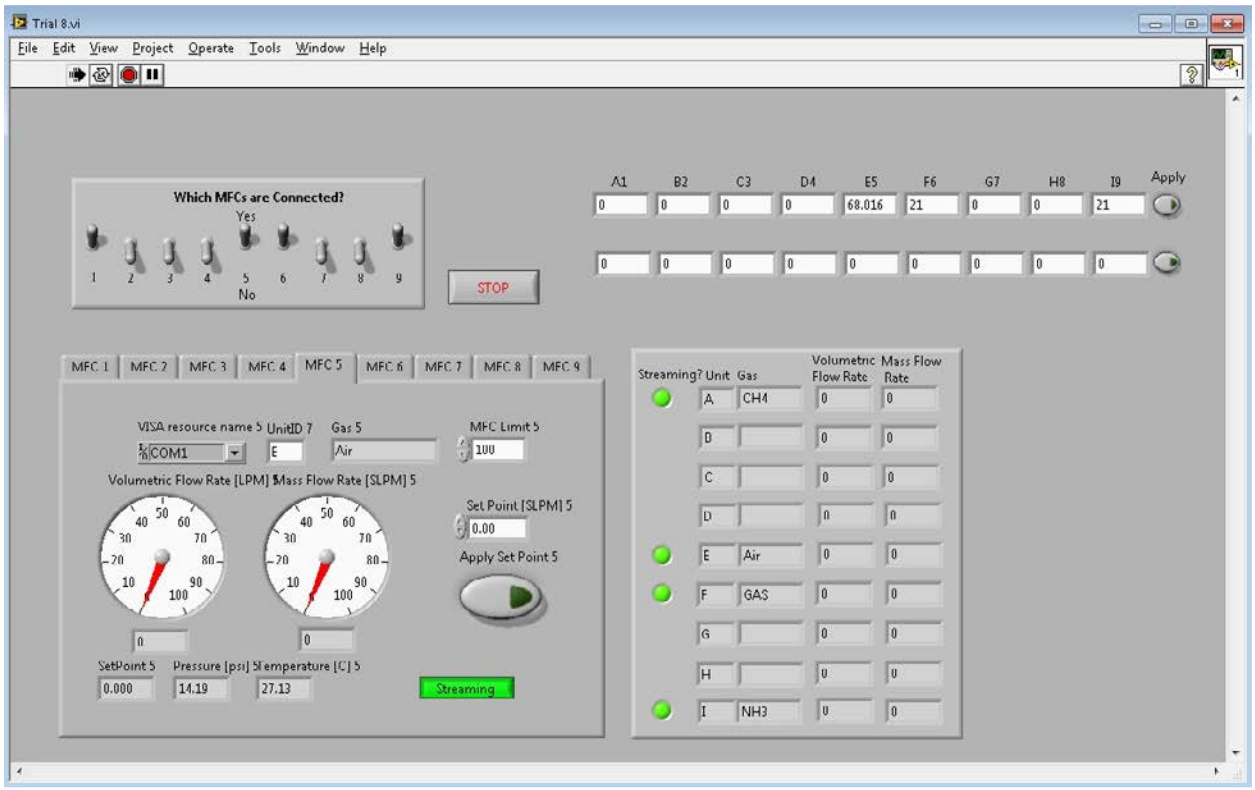

Figure 4.5 MFC control Labview program

4.4 Exhaust Measurement

Continuous exhaust samples and temperature measurements are taken from the combustion chamber at a location 23 inches above the injector head. The exhaust gas is first passed through a 120 micron screen filter to remove large particulate matter and then proceeds to enter a water and ammonia knock-out. Figures 4.6 and 4.7 show the knock-out, comprised of a series of three impingers sitting in a cold bath at 0℃. The first two impingers consist of a long stem submerged in ~120 mL deionized water. On the end of the stem, a metal sparger is mounted to promote the breakup of large bubbles to increase total area of the gas and promote the diffusion

of ammonia (as well as particulate matter) to the water. The third impinger is left empty and no sparger is present, which allows for the condensation of any remaining water before it leaves the impinger train.

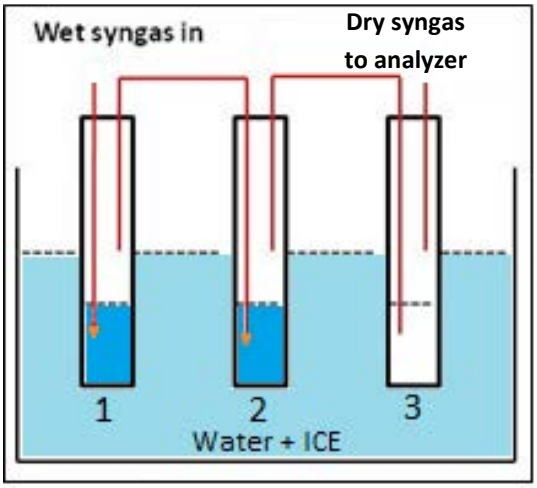

Figure 4.6 Impinger diagram

Figure 4.7 Impinger setup

The exhaust gas analyzer has a built-in vacuum pump in order to pull samples into the analysis chamber. However, this pump is not sufficient to pull the exhaust through the system of impingers, thus an additional vacuum pump is placed inline directly after the impinger train. From the pump, the exhaust is fed through a volumetric flow totalizer, and temperature and pressure readings are taken in order to calculate the total volume of exhaust flowed through the impinger trains to back calculate water and ammonia concentrations. After the flow meter, the conditioned gas passes through a five-gas analyzer manufactured by DeJaye Technologies. This analyzer can measure five different gas compounds, including CO, HC, and CO_2 using non-dispersive infrared (NDIR) technology and NO_x and O_2 using chemical cells. Figure 4.8 shows the gas cleanup and analysis section of the VUS combustion rig.

Figure 4.8 Gas cleanup and analysis

Once each test condition is run, the impinger train is removed from the exhaust gas system and the water is collected and filtered through a pre-weighed Whatman No. 40 filter paper, using a Buchner funnel vacuum system as shown in Figure 4.9. The sample is then collected in preweighed and labled 500 mL high density polyethylene bottle, taking a final weight to determine the amount of water that is collected through the combustion process. Once the filter paper has had sufficient time to dry, it is measured again and the weight of particulate collected is recorded. All water samples are stored in a dark refrigerator at approximately 32℃ immediately after collection to prevent the escape of ammonium contained in the sample.

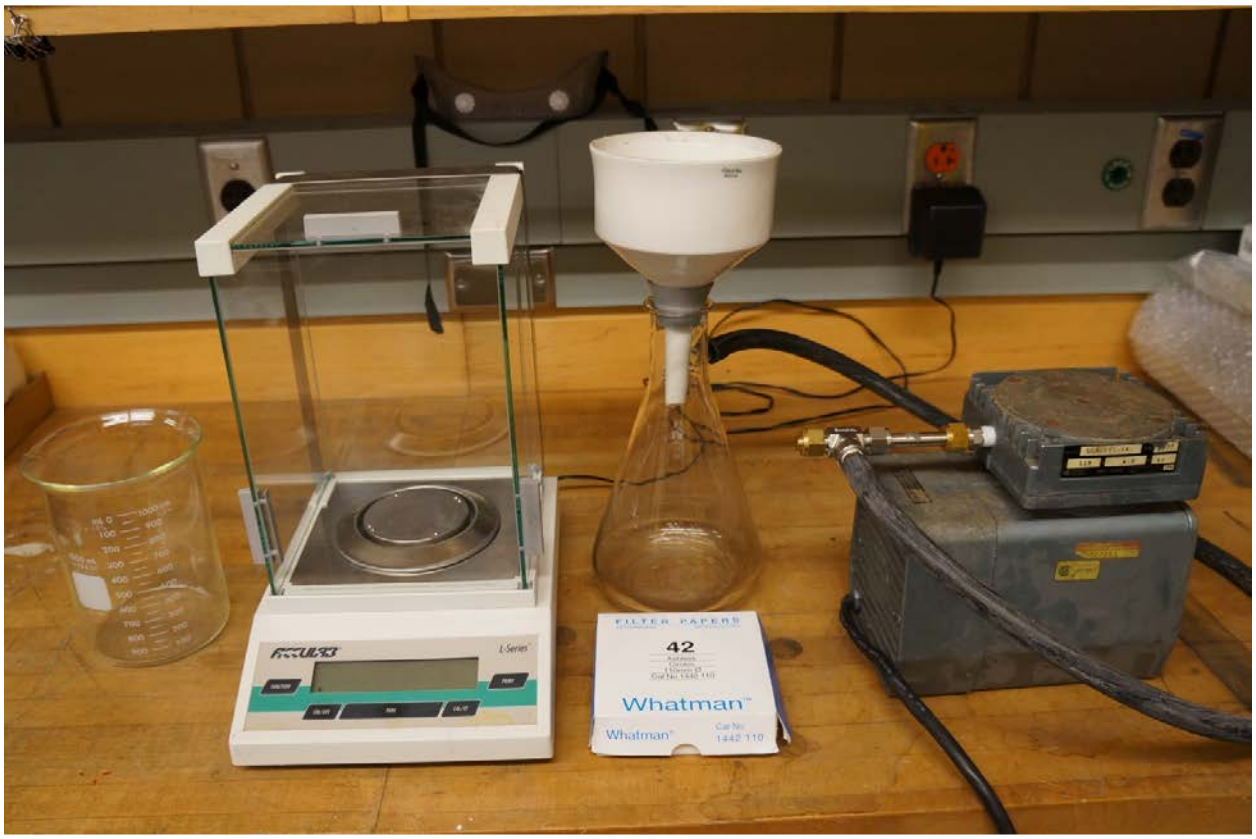

Figure 4.9 Impinger water collection and processing

Once sufficient samples have been collected, 20mL scintillation vials are then filled with the solution obtained from the impinger system. These vials are then submitted

to the Soil and Plant Analysis Laboratory to determine the amount of ammonium contained in each sample. This value is then used to back calculate the amount of ammonia contained in the exhaust gas.

Figure 4.10 Vials containing ammonia sample

The exhaust measurement system contains several limitations. Ammonium testing of the water samples should ideally be performed as soon as the test is run in order to ensure the most accurate results, but at a time period of no longer than one month after collection. Freezing the sample may allow for longer storage in extreme circumstances. Additionally, the DeJaye analyzer holds great benefit in this application due to the real time data observation it allows and ease of use. These benefits are coupled with the disadvantage of lower accuracies than other methods of gas analysis (Micro G.C., etc).

CHAPTER 5. RESULTS AND DISCUSSION

5.1 Process Model Results

An energy balance for this scenario shows that energy flow rate based on the lower heating value of the biomass is approximately 2.805 MMBTU/hr and the LHV of the producer gas is approximately 1.540 MMBTU/hr yielding an overall process energy efficiency of 59.8%. Note that this value is very high and results from a lack of details accounting for the additional energy required to operate this gasification plant including electricity and process heat for maintaining the boiler and biomass drying. Figures 5.1 and 5.2 compare the Aspen Plus model results to the experimental results obtained by Sethuraman, et al. (2011). The model is capable of predicting most component levels to a very good degree of certainty, with hydrogen being the overarching exception. As can be readily seen, the model over-predicts the yields of the various hydrocarbons and ammonia to a minimal amount, yet the sum of the hydrogen contained in this excess contributes to the discrepancy between molecular hydrogen in the model and with experimental results. It is believed that this difference exists because detailed kinetics are not considered in an RYIELD model, and therefore the Methane-Water Reforming reaction doesn't break down the hydrocarbons (i.e. methane) to carbon monoxide and elemental hydrogen. Despite the error in hydrogen, it is still believed that this model represents the actual gasification of wood quite well, and provides an excellent framework on which to model additional feedstocks for this gasifier. For additional feedstocks, biomass and producer gas compositions need only be replaced and then correlations for air

supplied to the gasifier and ratio of hydrogen converted to water vs molecular hydrogen need to be refined to simulate the actual process.

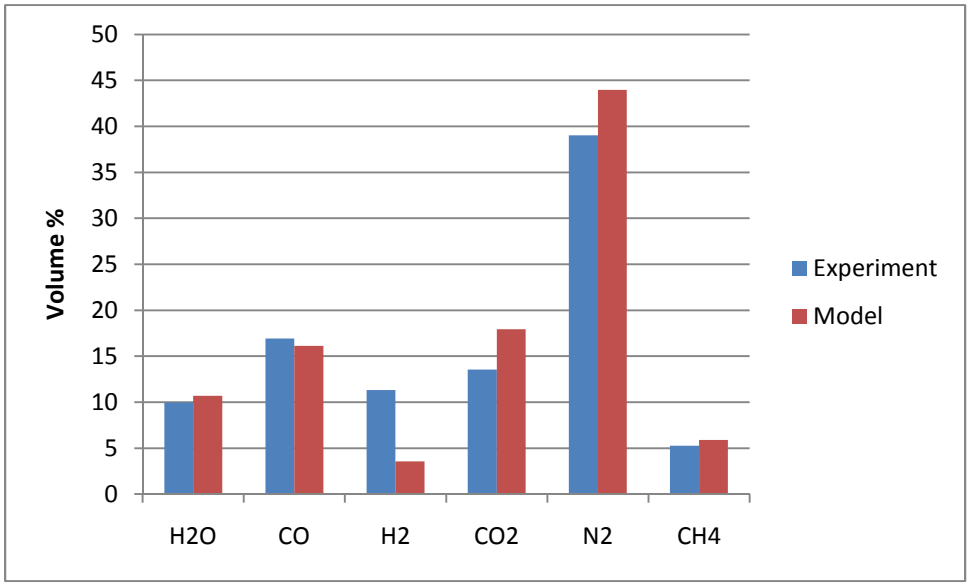

Figure 5.1 Comparison of Aspen Plus gasification model predictions with experimental results (Sethuraman, et al., 2011) **for major species**

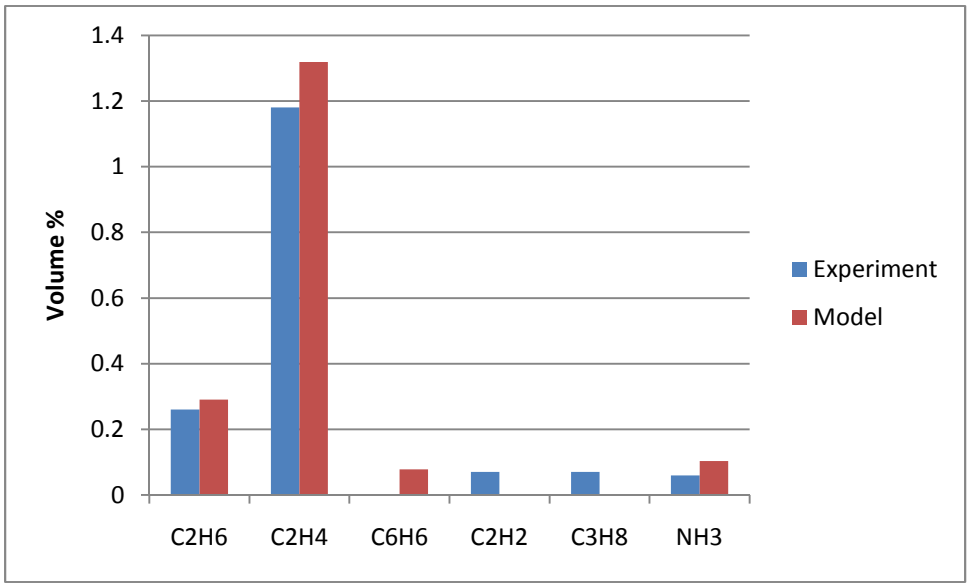

Figure 5.2 Comparison of Aspen Plus gasification model predictions with experimental results (Sethuraman, et al., 2011) **for minor species**

Figure 5.3 compares the Aspen Plus model combustion emissions with the experimental results for producer gas combustion (described in the next section). The model uses a stoichiometric method to calculate the theoretical combustion products. It should be noted that CO, CO_2, and O_2 are in terms of volumetric percent and NO_x is in parts per million. Results show good agreement for all components considered.

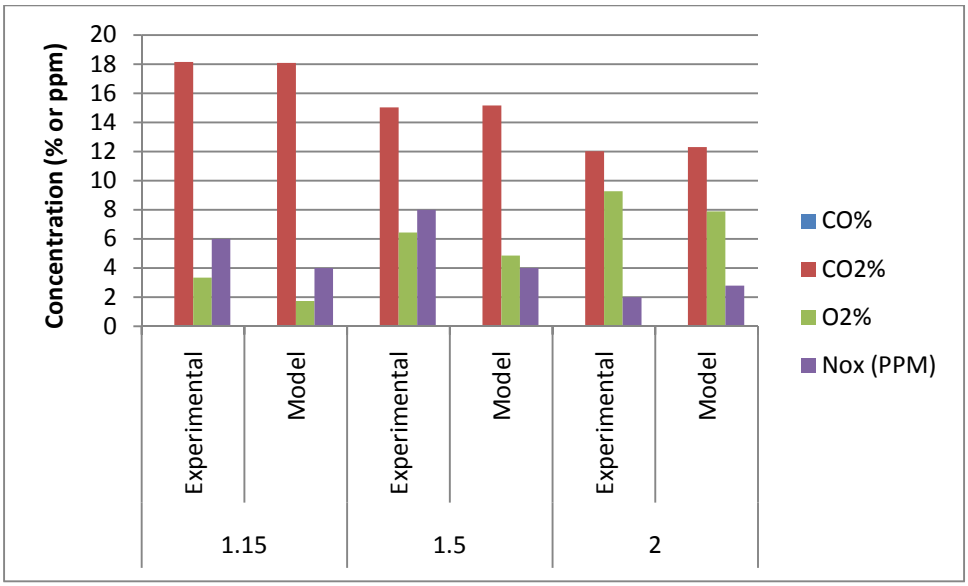

Figure 5.3 Comparison of Aspen Plus model predictions with lab-scale producer-gas emissions results

5.2 Experimental Combustion Results

5.2.1 Test Matrix

Combustion tests were conducted for natural gas and a 9 component producer gas which closely resembled the composition of the biomass derived producer gas reported by Sethuraman, et al. (2011). Initial tests were completed on the VUS

combustion rig utilizing in-house natural gas to ensure proper operation of the rig and gain valuable operating experience. During this time, operational data was taken utilizing each of the four swirlers (refer to Table 4.1) when it was decided to utilize the weakest swirl-strength swirler (number 1) in all subsequent trials due to the greater resolution of NO_x observed as a function of NH_3% in the fuel gas. All combustion test conditions were in the lean mixture range due to the temperature limitations of the combustion rig. Additionally, thermal NO_x becomes a major issue above 1800 K, so limiting this study to fuel-lean combustion processes allows for excess air to cool the flame and kept the flame temperature below 1800 K, characterizing the observed NO_x as primarily due to fuel NO_x. Once the operation and procedures of the VUS combustion rig were well understood, the test matrix was expanded to include additional equivalence ratios and ammonia concentrations for both natural gas and producer gas studies. A summary of the test conditions investigated can be found in Table 5.1.

Table 5.1 Test Conditions

Fuel	Swirler	Equivalence Ratio	NH_3 % in Fuel
Natural Gas	1, 2, 3, 4	1.15, 1.5	0, 0.006, 0.0213, 0.0353
Natural Gas	4	1.15, 1.5, 2.0	0, 0.06, 0.213, 0.353, 0.7, 1
Producer Gas	4	1.15, 1.5, 2.0	0, 0.06, 0.213, 0.353, 0.7, 1

5.2.2 Emissions Calculation Notes

Studies were conducted as described in Chapter 4 of this thesis. The 5-gas DeJaye analyzer provided concentrations of NO_x (PPM), CO%, CO2%, and O2% as measured in the exhaust. A set of water impingers was used to capture ammonia that was not reacted in the flame. Finally, accurate measurement of all flowrates, inputs (deionized water and gas streams), and products (char and ammonium in the impinger train) allowed for a detailed accounting of the experiment. The actual ammonia reacted was adjusted by the amount that was measured in the impinger train as detailed in Eq.(1) below.

$$NH_{3,consumed} = NH_{3,input} - NH_{3,slip} \quad (1)$$

where,

$$\boldsymbol{NH_{3,slip} = NH_4(PPM) * \frac{Water\ Sample\ in\ the\ Impinger\ (L)}{Produer\ Gas\ Flowed\ through\ the\ Impingers\ (L)}}$$

Additionally, the reported NO_x emissions data have been normalized based on a 3% oxygen level in the exhaust gas. This common practice in the burner industry takes into account the dilution effect under lean conditions. For example, at fuel-lean conditions, the measured NO_x emissions have been diluted by the excess air in the system and comparisons of various equivalence ratios can be skewed by this effect. This calculation is done using the following equation.

$$\boldsymbol{NO_x @\ 3\%\ O_2 = NO_x\ Raw\ Data * \frac{(1-0.03)}{(1-O_2\%)}} \quad (2)$$

The fuel and air used in this study do not begin mixing until after entering the combustion chamber. However, it is believed that due to the effects of the swirl on the flame, this flame has several characteristics of a premixed flame. Similar to a premixed flame, a correlation exists between NO_x emissions and the equivalence ratio of combustion. Additionally, it was observed that swirlers 3 and 4 which correspond to higher strength swirls were generally more stable, indicating a well-mixed flame.

The flow rate used for natural gas was 5 SLPM and for the producer gas was 21 SLPM in all experiments. This corresponded to a heat rate of 3.33 kW for natural gas and 2.24 kW for the producer gas. The lower heating values are 50,016 kJ/kg and 5,830 kJ/kg, respectively. Finally, the adiabatic flame temperatures are 2,223 K and 2,000 K for natural gas and producer gas, respectively, calculated from the EES code found in Appendix D.

5.2.3 Swirler Combustion Studies

Figure 5.4 shows the effect of swirler strength on the overall combustion process. Figure 5.4(a) corresponds to Swirler 1 that has the weakest swirl. Increasing strength is depicted from left to right, thus Figure 5.4(d) corresponds to Swirler 4 that has the strongest swirl. It should be noted that Figure 5.4(d) was taken with an increased zoom setting to show the details of the excess mixing, and has been scaled to correspond to Pictures (a-c) in terms of size. Figure 5.5 shows the NO_x emissions for all four swirlers using natural gas for equivalence ratios of 1.15 and 1.5 and various NH_3 percentages from 0 to 0.0353 %. These ammonia concentrations

were considerably lower than what was seen in the producer gas investigated in this study and were investigated for a two-fold purpose. First, these results allow for the investigation of swirl strength on NO_x emissions. Additionally, the test apparatus and collection equipment was tested to see if detection of differences in NO_x emissions was possible for very little NH_3. As can be seen, NO_x emissions decrease with greater swirl strength. It is believed that this is due to greater mixing of fuel and air that occurs and shifts the behavior of the flame closer to a premixed type configuration. Additionally, it can be seen that at low ammonia concentrations in the fuel, only minor differences in NO_x emissions can be observed due to the difference in equivalence ratio. The highest difference is observed for Swirler 4, noting that an equivalence ratio of 1.5 corresponds to higher NO_x emissions by approximately 10 ppm when compared to an equivalence ratio of 1.15. An equivalence ratio of 1.15 corresponds to the highest temperatures inside the combustor, which typically correspond to the highest thermal and fuel NO_x. However, as can be observed, an equivalence ratio of 1.15 corresponds to the lowest NO_x emissions. This is consistent with the work of Adouane, et al. (2003) which showed that NO_x emissions in a natural gas-fired, swirl burner are lowest with 4% excess O_2, which is most close to the equivalence ratio of 1.15 investigated in this study. Finally, in order to ensure that these results were applicable for larger ammonia percentages in the methane flame, swirlers 1 and 4 were tested for an expanded range of ammonia corresponding to a range of 0 to 1 vol% of the fuel as can be seen in Figure 5.6. These results show consistency with what was observed at lower concentrations.

Figure 5.4 Swirler comparisons at 5 SLPM natural gas, 0 NH_3%

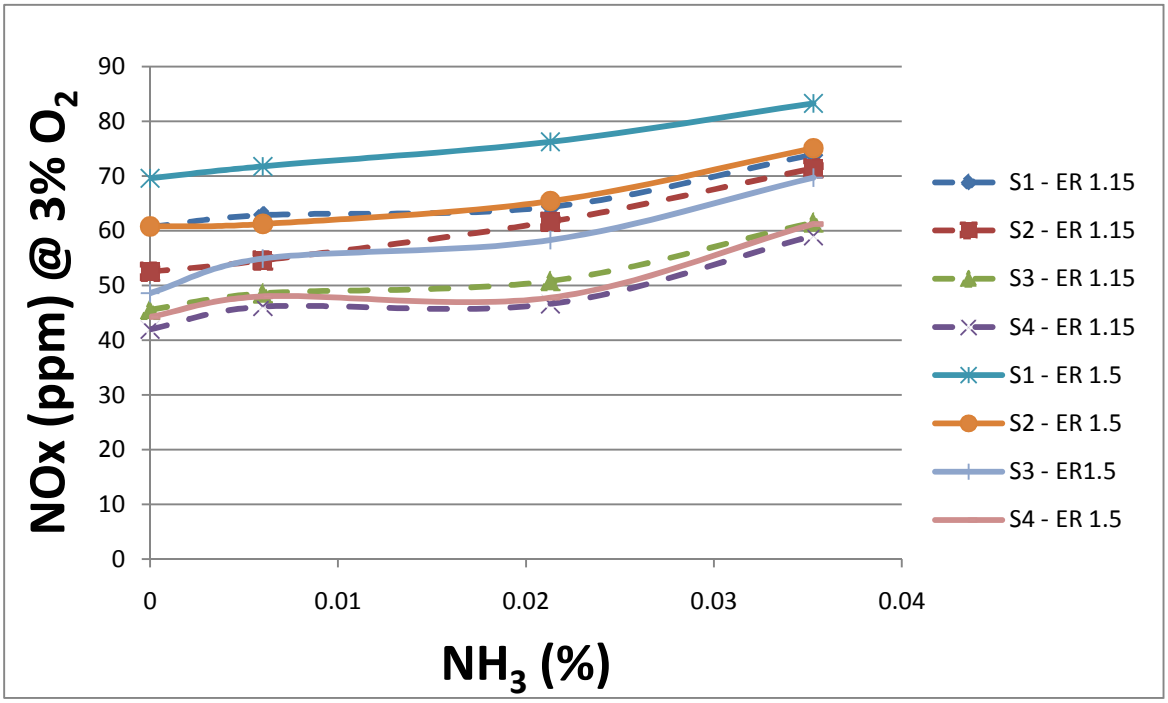

Figure 5.5 NO_x emission comparison of swirlers for natural gas at various equivalence ratios and low NH_3

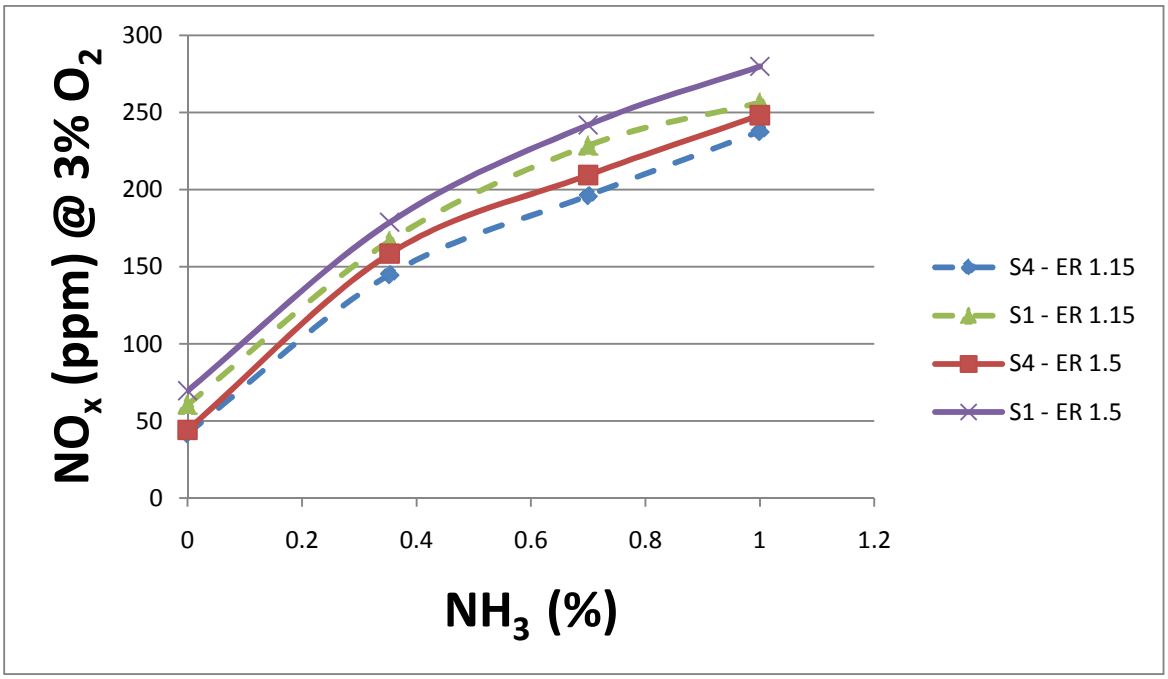

Figure 5.6 NO_x emission comparison of swirler 1 and 4 for natural gas at ER = 1.15 and 1.5 at various NH_x %

5.2.3 Natural Gas Combustion

Figure 5.7 shows the effect of increasing ammonia concentration for natural gas combustion at different equivalence ratios using swirler 1. These measurements represent the average data collected for two trials, beginning when steady conditions were reached for the DeJaye analyzer. Results for all trials showed very good agreement. As can be seen, for each equivalence ratio a direct relationship exists between the fuel-nitrogen and the NO_x emissions. Additionally, this relationship appears to resemble a log-relationship where there is a lower NO_x to NH_3 ratio at higher concentrations. This shows good agreement with the NH_3 – NO reduction mechanism illustrated in the bottom half of Figure 2.3. Finally, it is noted that equivalence ratios of 1.15 and 1.5 continue to follow the trend that NO_x emissions

are minimized with 4% excess air as observed in Section 5.2.2. At an equivalence ratio of 2.0 this same trend is not observed for natural gas. It is believed that this is due to the excess air reducing the overall temperature in the combustion chamber and thus reducing the thermal and fuel NO_x present at lower equivalence ratios.

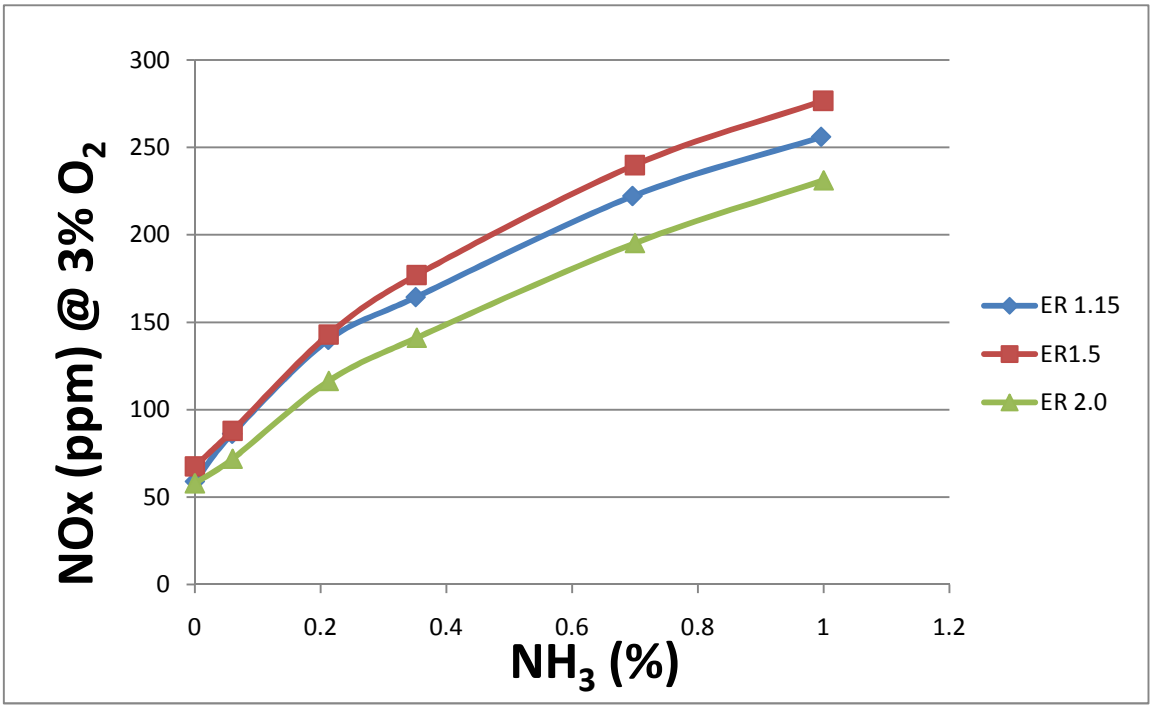

Figure 5.7 NO_x emissions for natural gas at 5 SLPM at various ER and NH_3%

5.2.3 Producer Gas Combustion

Figure 5.8 depicts producer gas combustion at an equivalence ratio of 1.15 and flowrate of 21 SLPM for swirler 1 (Figure 5.8(a)) and swirler 4 (Figure 5.8(b)). It can be seen from the photos that the higher swirl strength of swirler 4 produces a more compact and stable flame compared to swirler 1. This increase in stability results in more complete combustion and overall lower NO_x emissions. Figure 5.9 shows the effect of increasing NH_3 concentrations on NO_x emissions. It can be seen that

higher equivalence ratios correspond to lower NO_x. This can be attributed to several phenomena. The adiabatic flame temperature of producer gas is approximately 200 K lower than that of natural gas. Thus, the effect of thermal NO_x is lower. Additionally, these lower temperatures provide less overall energy in the system that is available to drive the fuel NO_x production. Therefore, the production of fuel NO_x is low. Next, in order to obtain a heat rate on the same order as was used for natural gas, this combustor had to be operated near the peak of its input capabilities for this injector. In fact, the flame was not stable at the same heat rate of the natural gas experiments because the gas velocity was too much too high to allow for steady combustion. Thus, a lower heat rate was chosen to carry out the producer gas experiments. At higher equivalence ratios, combustion air velocities increased greatly which resulted in a very short residence time for the flame. Shorter residence times result in lower fuel-NO_x emissions. Finally, the excess air required for higher equivalence ratios had an overall thermal dilution effect on the flame, thus cooling the flame and resulting in lower thermal NO_x with higher equivalence ratios. Factoring in reductions in thermal NO_x and fuel NO_x at higher equivalence ratios accounts for the results observed for the producer gas combustion corresponding to lower NO_x emissions with increasing equivalence ratios. The final observation is that the relationship between NH_3 and NO_x is much more linear than that of natural gas, thus showing that the NH_3 – NO reduction illustrated in Figure 2.3 has less of an effect under the conditions of producer gas combustion shown here.

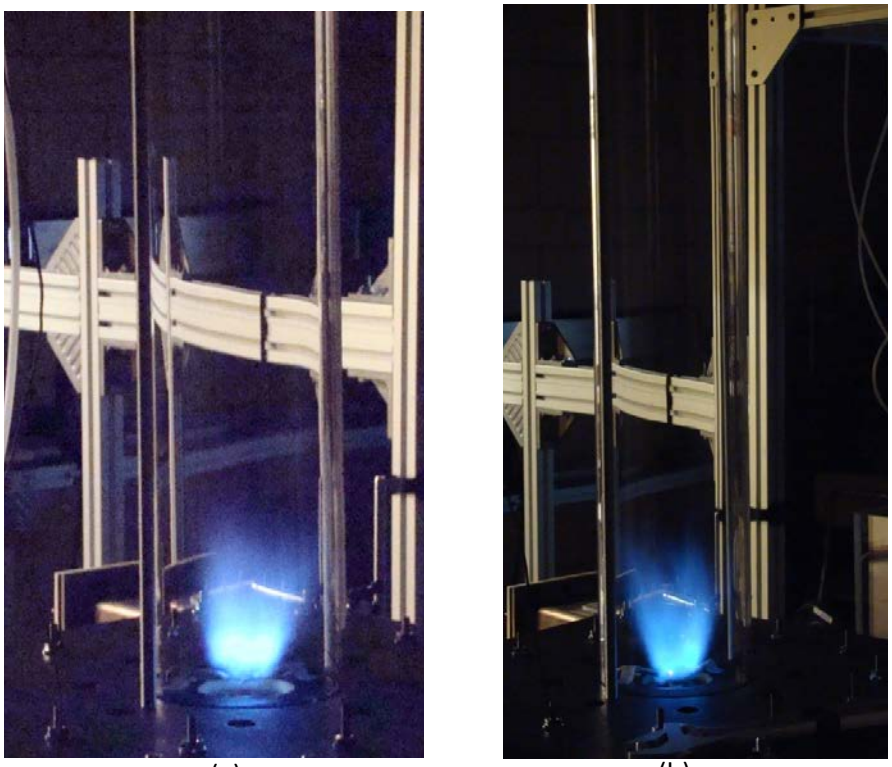

(a) (b)

Figure 5.8 Comparison of swirler 1 (a) and swirler 4 (b) at 21 SLPM producer gas, 0 NH_3%

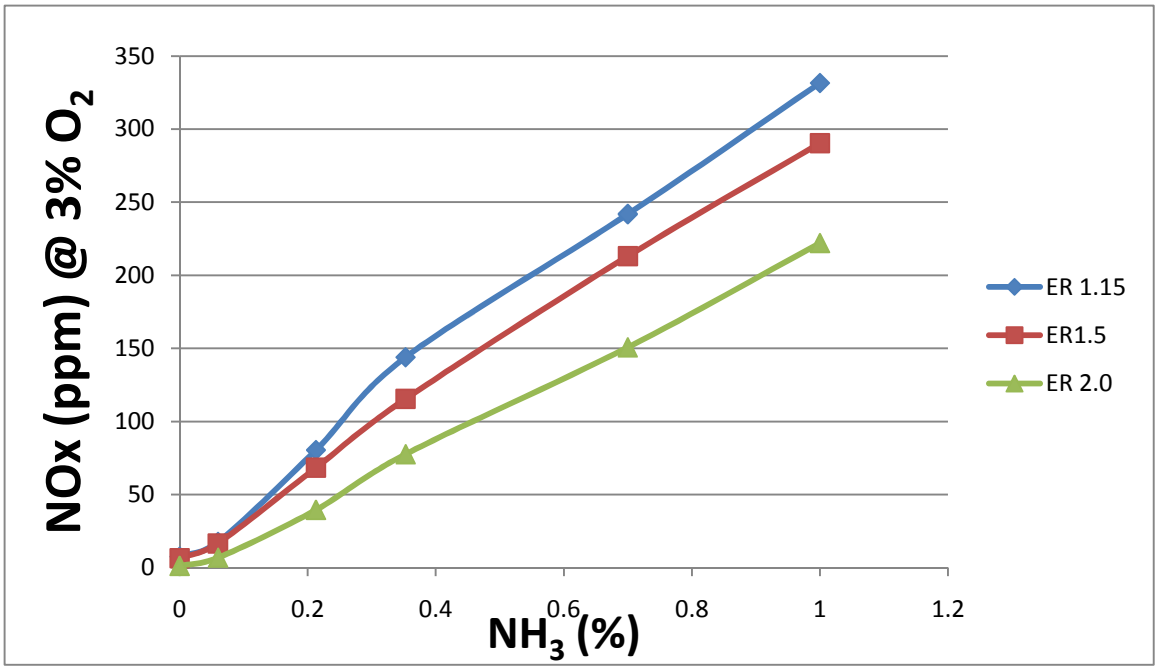

Figure 5.9 NO_x emissions for producer gas at 21 SLPM at various ER and NH_3%

5.2.4 Discussions

There were a few issues that arose during the testing phase including high soot levels in the natural gas flames and flammability issues with the low heating value producer gas. Due to the nature of non-premixed combustion of hydrocarbon fuels, soot becomes an issue in a natural gas flame. This soot led to build-up on the combustion chamber walls, within the exhaust sampling lines, in the water knock-out, and eventually if not managed properly, within the gas analysis equipment. A swagelok 90-micron screen filter was used as a primary filter as soon as the gas was sampled. The gas then passed through the impinger train where further particles were captured either by the spargers or the water. Finally, two automotive gasoline filters were placed in series before the DeJaye gas analyzer to ensure a particulate free sample entered. After each run, the impinger train was dismantled, the sample was collected, and all soot was washed from the system. Additionally, the 90 micron filter had to be cleaned with water after each test run for the natural gas tests. The automotive filters were replaced as needed which was generally as often as once per day.

The low heating value and high nitrogen content of the producer gas led to flammability issues in the producer gas. Very high flow rates of both producer gas and air were required in order to obtain the same heat rate as was necessary to see any effect of swirl on the natural gas flame. These high flow rates in the injector/swirler system being used led to very high velocities which the flame speed could not keep up with. In order to ensure a stable flame for the experiment, a heat rate roughly one-third lower had to be used for the producer gas combustion. The

producer gas burned much cleaner than the natural gas and soot was not an issue for these tests.

The relationship between equivalence ratio and NO_x emissions was observed to be different for natural gas and producer gas. This can be explained by the different chemistries that exist with each fuel source. Natural gas is composed almost entirely of methane and has an adiabatic flame temperature around 2223 K allowing for the production of thermal NO_x for various regions within the swirling flame. Additionally, it is known that a natural gas flame that lowest NO_x emissions occur at an equivalence ratio of around 1.15. The characteristics of producer gas on the other hand are entirely dependent on the composition of the gas and are not well understood. The producer gas used in this study has an adiabatic flame temperature of around 2,000 K, which results in less of an effect of thermal NO_x. Lower heating values require a much higher flowrate of gas which increases the velocity and lowers the residence time, thus reducing fuel NO_x. The differences in the NO_x mechanisms between both fuels used in this study illustrate how important a full understanding of the fuel being used is when trying to reduce overall NO_x, and proves motivation for the need of vastly greater study into the combustion of low heating value producer gas for low-swirl burners.

CHAPTER 6. CONCLUSIONS AND RECOMMENDATIONS

6.1 Conclusions

An Aspen Plus process model was created to simulate the production, cleanup, and combustion of a producer gas created from the gasification of wood. With the exception of hydrogen in the producer gas, this model was able to accurately predict the producer gas composition based on an elemental balance approach. Additionally, the stoichiometric combustion model predicted the resulting exhaust within acceptable limits compared to the lab scale experiments conducted in this thesis.

Experiments were conducted on a lab scale, low-swirl burner combustion system using natural gas and a 9 component producer gas as fuel sources. Equivalence ratio and ammonia concentration were the major variables investigated along with a basic study that varied swirl strength in a natural gas flame. Four swirlers with effective flow areas ranging from 1.52 to 2.0 in^2 were used to study the effect of swirl strength on the Fuel-N to NO_x relationship.

This study was able to establish a relationship between the ammonia content in a gaseous fuel to the fuel NO_x formation in the burner. Furthermore, equating the ammonia content in the producer gas as proportional to the nitrogen found in the biomass feedstock prior to gasification, a relationship between feedstock nitrogen content and producer gas NO_x emissions has been established. The effect of swirl strength varies inversely with NO_x emissions. It is believed that increased mixing

and recirculation within the turbulent swirl region allows for higher residence time which in turn reduced the fuel NO_x.

6.2 Recommendations

The overall objective of this study was to develop a biomass gasification model that predicted producer gas composition to a good degree of accuracy for a given feedstock and to study the effect of ammonia concentration on overall NO_x emissions when the producer gas was combusted. As can be observed in literature, both of these concepts are worthy of considerable study among the entire scientific community and thus the scope of this thesis was not able to cover every detail. It is recommended that improvements be made to the Aspen Plus model in three main areas. First, a detailed kinetic model should be developed that is capable of predicting the producer gas composition for a much wider variety of feedstocks. The current model is limited in the scope of the feedstocks it can handle, as has been seen a common occurrence in literature. Second, a detailed pinch analysis should be completed to ensure an accurate accounting of all heat and energy streams in the system. Finally, the areas other than the gasification block are not modeled rigorously and can be improved by implementing a more detailed gas cleanup and combustion kinetics model.

The study of low-swirl burners is still in its infancy and has called for the expansion of the current understanding and knowledge. As such, different fuels, equivalence ratios, and swirlers should be further studied to better understand the details behind producer gas combustion in low-swirl burners.

BIBLIOGRAPHY

Adouane, B., Witteveen, G., de Jong, W., van Buijtenen, J., Towards the Design of an Ultra Low NOx Combustor for Biomass Derived LCV Gas. Rev. Energ. Ren: 11th Journees Internationales de Thermique, 2003, 111-117.

Bain, R. L., Material and Energy Balances for Methanol from Biomass Using Biomass Gasifiers. National Renewable Energy Laboritory. NREL/TP-510-17098, 1992.

Basu, P., Biomass Gasification and Pyrolysis: Practical Design and Theory. Elsevier Inc 2010.

Bhoi, P. R., Channiwala, S. A., Emission charachteristics and axial flame temperature distribution of producer gas fired premixed burner. Biomass and Bioenergy: 2009, 33, 469 - 477.

Bhoi, P. R., Channiwala, S. A., Optimization of producer gas fired premixed burner. Renewable Energy 2008, 33, 1209 - 1219.

Brown, R. C., Biorenewable resources: engineering new products from agriculture. Iowa State Press: Ames, Iowa, 2003.

Ciferno, J. P., Marano, J. J., Benchmarking Biomass Gasification Technologies for Fuels, Chemicals and Hydrogen Production. US Department of Energy, National Energy Technology Laboratory, 2002.

Consonni, S., Larson, E. D., Biomass-Gasifier/Aeroderivative Gas Turbine Combined Cycles: Part A—Technologies and Performance Modeling. Journal of Engineering for Gas Turbines andd Power: July, 1996, 118.

Doherty, W., Reynolds, A., Kennedy, D., Simulation of a circulating fluidised bed biomass gasifier using ASPEN Plus - a performance analysis. 21st international conference on efficiency, cost, optimisation, simulation, and environmental impact of energy systems: 2008, 1241-1248.

EIA, Energy Information Administration, Annual Energy Outlook 2011 with Projections to 2035, 2011.

EPA, Environemntal Protection Agency, EPA Proposes First Carbon Pollution Standard for Future Power Plants, 2012.

EPA, Environmental Protection Agency, Regulation of Fuels and Fuel Additives: Changes to Renewable Fuel Standard Program: Rules and Regulations: Federal Register, 2010, 75, (58).

Fotache, C. G., Tan, Y., Sung, C. J., Law, C. K., Ignition of CO/H2/N2 versus heated air in counterflow: experimental and modeling results. Combustion and Flame, 2000, 120, (4), 417 - 426.

Greene, D. L., Measuring energy security: Can the United States achieve oil independence? Energy Policy. April, 2010, 38, (4), 1614 - 1621.

Hannula, I., Kurkela, E., A semi-mpirical model for pressurised air-blown fluidised-bed gasification of biomass. Bioresource Technology, June, 2010, 101, (12), 4608 - 4615.

Kirkels Arjan F and Verbong Geert P.J. Biomass gasification: Still promising? A 30-year global overview. Renewable and Sustainable Energy Reviews, January, 2011, 15, (1), 471-481.

Kumar A., Jones D. D., Hanna, M. A., Thermochemical Biomass Gasification: A Review of the Current Status of the Technology. Energies, 2009, 556-581.

Li, C-Z., Tan, L. L., Formation of NOx and SOx precursors during the pyrolysis of coal and biomass. Part 3. Further discussion on the formation of HCN and NH3 during pyroloysis. Fuel, 2000, 79, (15), 1899-1906.

Li, X. T., Grace, J. R., Lim, C. J., Watkinson, A. P., Chen, H. P., Kim, J. R., Biomass gasification in a circulating fluidized bed. Biomass and Bioenergy, 2004, 26, (2), 171-193.

Lieuwen, T., McDonell, V., Petersen, E., Santavicca, D., Fuel Flexibility Influences on Premixed Combustor Blowout, Flashback, Autoignition, and Stability. Journal of Engineering for Gas Turbines and Power, January, 2008, 130.

Lieuwen, T., Yang, V., Yetter, R., Synthesis Gas Combustion: Fundamentals and Applications. Taylor & Francis: Boca Raton, FL, 2010.

Littlejohn, D., Cheng, R. K., Noble, D. R., Lieuwen, T., Laboratory Investigations of Low-Swirl Injectors Operating with Syngases. Journal of Engineering for Gas Turbines and Power. January, 2010, 132.

Mandl, C., Obernberger, I., Scharler, I. R., Characterisation of fuel bound nitrogen in the gasification process and the staged combustion of producer gas from the updraft gasification of softwood pellets. Biomass and Bioenergy, 2011, 35, 4595 - 4604.

Marban, G., Valdes-Solis, T., Towards the hydrogen economy? International Journal of Hydrogen Energy, 2007, 32, (12), 1625 - 1637.

McKendry, P., Energy production from biomass (part 3): gasification technologies. Bioresource Technology. May, 2002, 83, (1), 55-63.

Nikoo, M. B., Mahinpey, N., Simulation of biomass gasification in fluidized bed reactor using ASPEN PLUS. Biomass and Bioenergy, 2008, 32, 1245 - 1254.

Panwar, N. L., Salvi, B. L., Reddy, V. S., Performance evaluation of produce gas burner for industrial application. Biomass and Bienergy, 2011, 35, 1373 - 1377.

Perlack, R. D., Wright, L. L., Turhollow, A. F., Graham, R. L., Stokes, B. J., Erbach, D. C., Biomass as feedstock for a bioenergy and bioproducts industry: the technical feasibility of a billlion-ton annual supply. US DOE and USDA, 2005.

Proll, T., Hofbauer, H., H2 rich syngas by selective CO2 removal from biomass gasification in a dual fluidized bed system - Process modeling approach. Fuel Processing Technology. November, 2008, 89, (11), 1207-1217.

Puig-Arnavat, M., Bruno, J. C., Coronas, A., Review and analysis of biomass gasification models. Renewable and Sustainable Energy Reviews, 2010, 14, 2841 - 2851.

Ribert, G., Thakre, P., Wang, Z., Yetter, R. A., Yang, V., Fundamental Combustion Charachteristics of Syngas - Synthesis Gas Combustion: Fundamentals and Applications. Edit: Lieuwen, T., Yang, V., Yetter, R., 2010.

Sarofim, A. F., Pohl, J. H., Taylor, B. R., Strategies for Controlling Nitrogen Oxide Emissions During Combustion of Nitrogen-Bearing Fuels. AIChE Symposium Series, 1978, 74(175), 67-92.

Sethuraman, S., Van Huynh, C., Kong, S-C., Producer Gas Composition and NOx Emissions from a Pilot-Scale Biomass Gasification and Combustion System Using Feedstock with Controlled Nitrogen Content. Energy and Fuels, 2011, 25, 813-822.

Spath, P. L., Dayton, D. C., Preliminary Screening - Technical and Economic Assessment of Synthesis Gas to Fuels and Chemicals with Emphasis on the Potential for Biomass-Derived Syngas. National Renewable Energy Laboratory, 2003.

Sullivan, N., Jensen, A., Glarborg, P., Day, M. S., Grcar, J. F., Bell, J. B., Pope, C. J., Kee, R. J., Ammonia Conversion and NOx Formation in Laminar Coflowing Nonpremixed Methane-Air Flames. Combustion and Flame, 2002, 131, (3), 285-298.

Sung, C-J., Law, C. K., Fundamental Combustion Properties of H2/CO Mixtures and Flame Propagation at Elevated Pressures. Combust. Sci. and Tech., 2008, 180, 1097 - 1116.

Surjosatyo, A., Priambodho, Y. D., Investigation of Gas Swirl Burner Characteristic on Biomass Gasification System using Combustion Unit Equipment (CUE). Jurnal Mekanikal. December, 2011, 33, 15-31.

Swanson, R. M., Satrio, J. A., Brown, R. C., Platon, A., Hsu, D. D., Techno-Economic Analysis of Biofuels Production Based on Gasification. National Renewable Energy Laboratory. NREL/TP-6A20-46587, 2010.

Tan, W., Zhong, Q., Simulation of hydrogen production in biomass gasifier by ASPEN PLUS. IEEE, 2010, 10, 1-4.

Tian, F-J., Yu, J., McKenzie, L. J., Hayashi, J-i., Li, C-Z., Conversion of Fuel-N into HCN and NH3 During the Pyrolysis and Gasification in Steam: A Comparative Study of Coal and Biomass. Energy and Fuels, 2007, 21, 517 - 521.

Turns, S. R., An Introduction to Combustion: Concepts and Applications. McGraw Hill, 2000.

Wang, L., Weller, C. L., Jones, D. D., Hanna, M. A., Contemporary issues in thermal gasification of biomass and its application to electricity and fuel production. Biomass and Bioenergy, 2008, 32, 573-581.

Whitty, K. J., Zhang, H. R., Eddings, E. G., Pollutant Formation and Control - Synthesis Gas Combustion: Fundamentals and Applications, Edit: Lieuwen, T., Yang, V., Yetter, R., Taylor& Francis Group: Boca Raton, FL, 2010.

Yu, Q., Brage, C., Chen, G., Sjostrom, K., The fate of fuel-nitrogen during gasification of biomass in a pressurised fluidised bed gasifier. Fuel, 2007, 86, 611-618.

Zhou, J., Masutani, S. M., Ishimura, D. M., Turn, S. Q., Kinoshita, C. M.,Release of Fuel-Bound Nitrogen during Biomass Gasification. Industrial & Engineering Chemistry Research,2000, 39, 626-634.

Zhou, L. X., Chen, X. L., and Zhang J., Studies on the effect of swirl on NO formation in methane/air turbulent combustion. Proceedings of the Combustion Institute, 2002, 29, 2235-2242.

APPENDIX A. SCENARIO MODELING DETAILS

A.1 Property Method

The model operates globally with the Redlich-Kwong-Soave with Boston –Mathias modification (RKS-BM) property method which is recommended in the program for use in medium temperature refining and gas processing including combustion and gasification. Additionally, in order to better estimate the solids simulations for the cyclone operation, the model setup includes a particle size distribution.

A.2 Aspen Plus™ Calculator Block Descriptions

EFF

This block calculates the gasification energy efficiency between the total energy entering the plant in the biomass and the amount of energy possible in the producer gas. This is done on both the HHV and LHV basis and is simply defined as the ratio of producer gas HV to biomass HV for both the higher and lower heating value basis.

GASYIELD

This model uses an elemental balance approach to calculate the product distribution which results from the gasifier. Experiments performed at the BECON research facility provide the initial gasifier product distribution, and a calculation block adjusts these parameters in order to balance all species.

The approach taken to balance each element (carbon, hydrogen, oxygen, sulfur, nitrogen, and ash) is to have a “floating” component for each element. This component’s yield is adjusted in order to meet the demands of the rest of the process. For example, char is used to “float” carbon. If there is insufficient carbon in the other process streams, less char is produced and the excess carbon is distributed where needed. After carbon is balanced, the calculation proceeds to sulfur and nitrogen balances, with any excess being converted to form hydrogen sulfide and ammonia. Next, elemental hydrogen is adjusted to fit the operating conditions by either converting diatomic hydrogen to steam or decomposing steam to diatomic hydrogen. A scaling factor can be implemented in this step to determine the amount of diatomic hydrogen that gets converted to steam to best match experimental results. Finally, oxygen is balanced by adjusting the amount of CO_2 and CO which exit the gasifier.

Details of this method can be found in (Swanson, et al., 2010).

HV-101 and HV-203

This block calculates the lower and higher heating values for biomass and syngas, respectively. These values are used in calculating

O2COMB

This block calculates the amount of air that is required to combust with the producer gas under stoichiometric conditions. The reactions are as follows in Table A.1.

Table A.1 Combustion reactions to determine required oxygen

Component	Reaction
CO	$CO + 0.5*O_2 \rightarrow CO_2$
H2	$H_2 + 0.5*O_2 \rightarrow H_2O$
CH4	$CH_4 + 2*O_2 \rightarrow 2*H_20 + 2*CO_2$
C2H6	$C_2H_6 + 3.5*O_2 \rightarrow 3*H_2O + 2*CO_2$
C2H4	$C_2H_4 + 3*O_2 \rightarrow 2*H_2O + 2*CO_2$
C6H6	$C_6H_6 + 7.5*O_2 \rightarrow 3*H_2O + 6*CO_2$
C3H8	$C_3H_8 + 5*O_2 \rightarrow 4*H_2O + 3*CO_2$
H2S	$H_2S + 1.5*O_2 \rightarrow H_2O + SO_2$
NH3	$NH_3 + 1.75*O_2 \rightarrow 1.5*H_2O + NO_2$
TAR	$C_{14}H_{10}$ (*tar*) $+ 16.5*O_2 \rightarrow 5*H_2O + 14*CO_2$

The molar flow rate of oxygen entering the combustor is summed and multiplied by a factor of "a" in order to obtain the percent excess oxygen used during combustion. Values used in this model correspond to a = 1.15 to 2.0, corresponding to 15% to 100% excess oxygen according to the equation below.

$$\dot{M}_{O2,in} = a * (0.5\dot{M}_{CO} + 0.5\dot{M}_{H2} + 3.5\dot{M}_{C2H6} + 3\dot{M}_{C2H4} + 7.5\dot{M}_{C6H6} + 5\dot{M}_{C3H8} + 1.5\dot{M}_{H2S} + 1.75\dot{M}_{NH3} + 16.5\dot{M}_{TAR}) \quad \text{(A.1)}$$

$$\dot{M}_{N2,in} = \dot{M}_{O2,in} * \left(\frac{0.79}{0.21}\right) \quad \text{(A.2)}$$

OXYSET

This block sets the amount of air entering the gasifier as a function of the feed rate of biomass in according to the following equations:

$$\dot{m}_{O2,gas} = c * \dot{m}_{biomass} \quad \text{(A.3)}$$

$$\dot{m}_{N2,gas} = \left(\frac{0.79}{0.21}\right) * \dot{m}_{O2,gas} \quad \text{(A.4)}$$

where c is one parameter in the model that is modified to better simulate experimental data.

APPENDIX B. PROCESS FLOW DIAGRAMS

Figure B.1 General Gasification Scenario

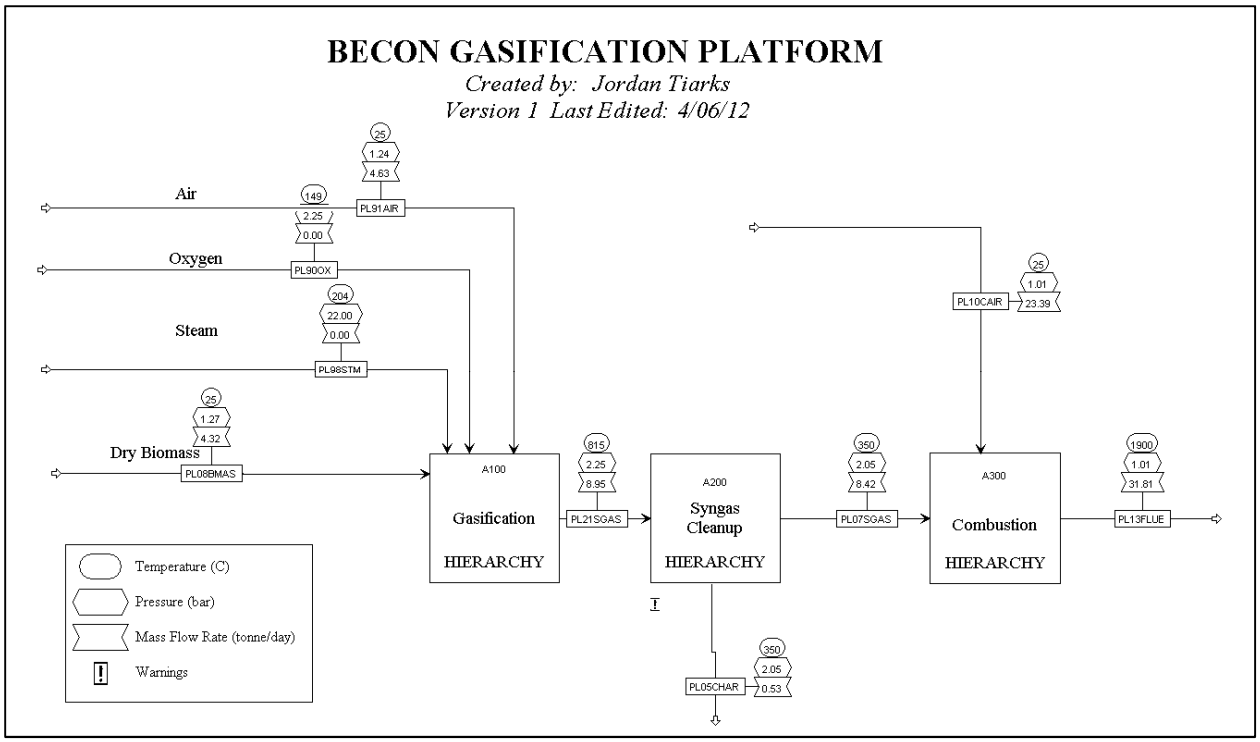

Figure A.2 Area 100 Gasification Reactor

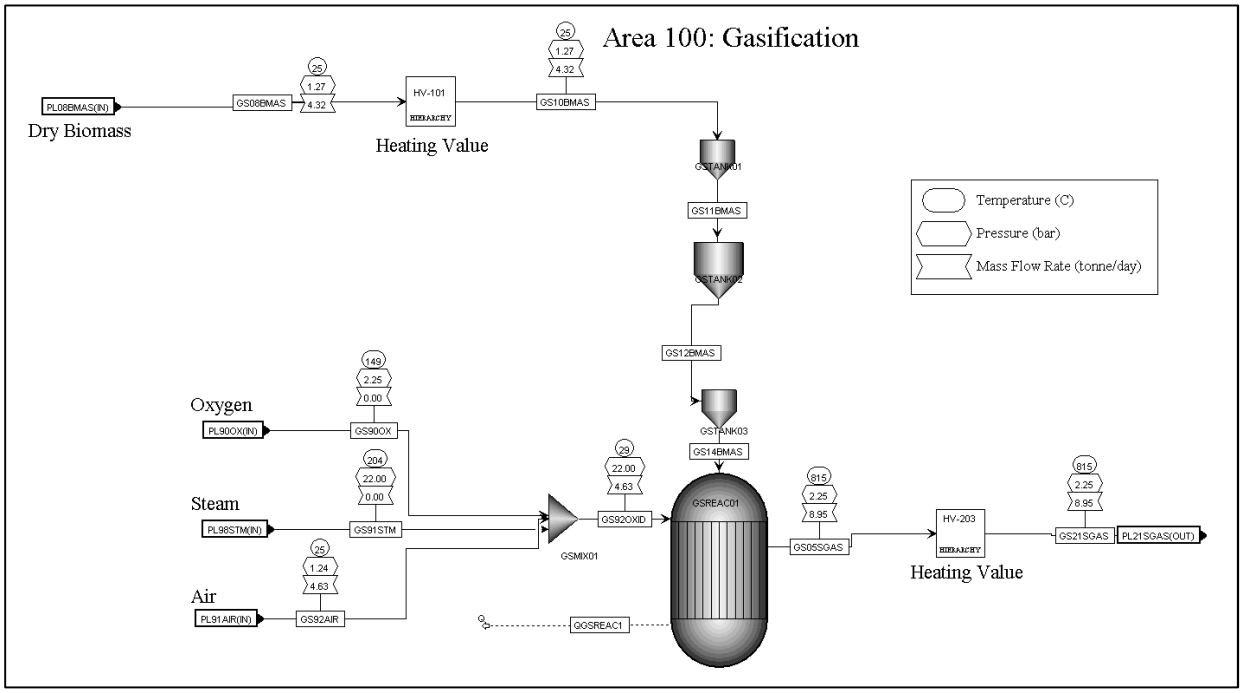

Figure B.3 Area 200 Gas Cleanup

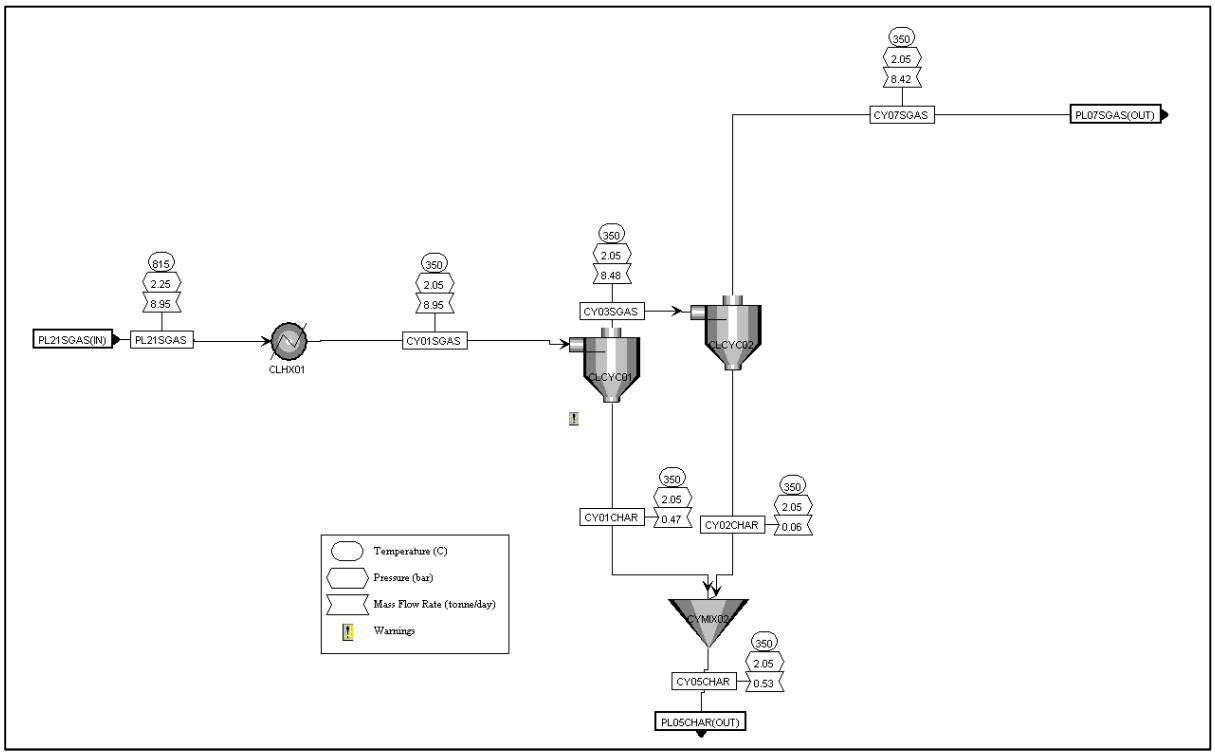

Figure B.4 Area 300 Combustion

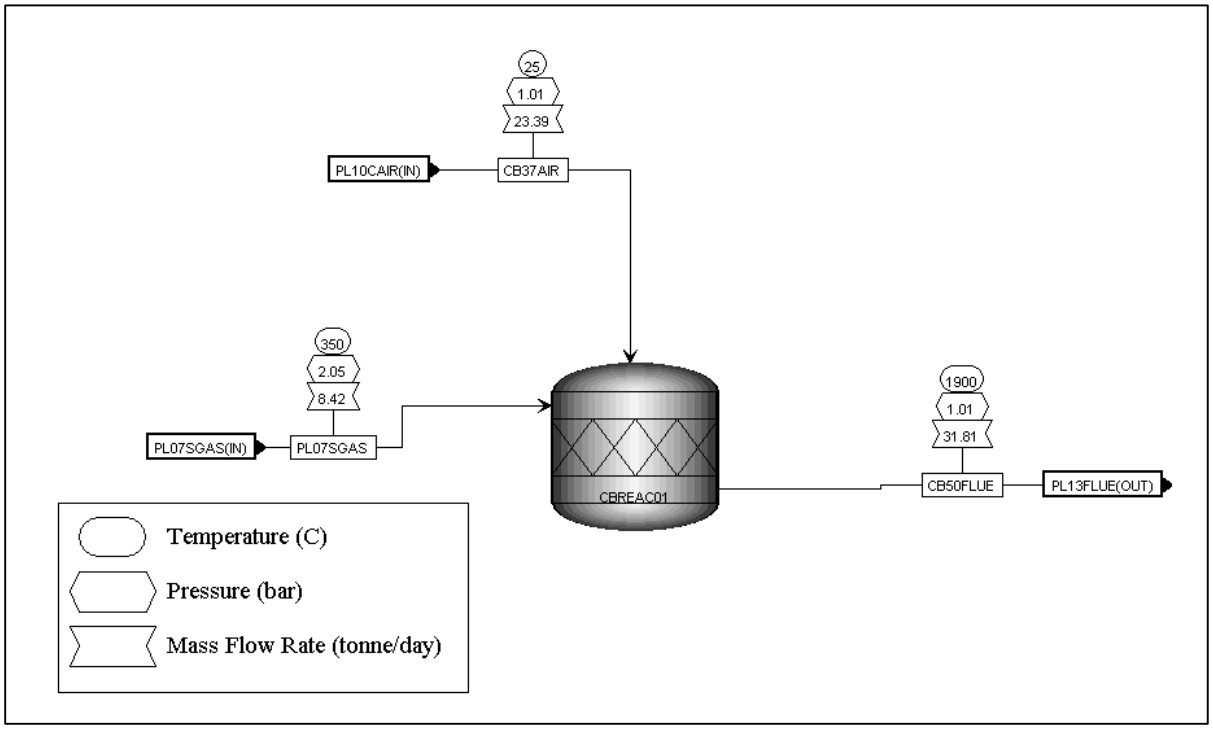

Table C.1 Overall Stream Data

Overall Plant	PL05CHAR	PL07SGAS	PL08BMAS	PL10CAIR	PL13FLUE	PL21SGAS	PL90OX	PL91AIR	PL98STM
Temperature (°C)		350	25	25	1900	815	148.89	25	204.44
Pressure (bar)	2.05	2.05	1.27	1.01	1.01	2.25	2.25	1.24	22
Vapor Fraction		1	0	1	1	1	1	1	0
Volume Flow ** (m^3/sec)	0	0.09	0	0.23	2.23	0.14	0	0.04	0
Mole Flow ** (kmol/hr)	0	12.38	0.62	33.78	44.97	12.38	0	6.7	0
Mass Flow (tonnes/day)	0.53	8.42	4.32	23.39	31.81	8.95	0	4.63	0
H2O	0	0.57	0.27	0	1.62	0.57	0	0	0
CO	0	1.34	0	0	0	1.34	0	0	0
H2	0	0.02	0	0	0	0.02	0	0	0
CO2	0	2.35	0	0	5.85	2.35	0	0	0
O2	0	0	0	5.45	2.72	0	0	0.97	0
N2	0	3.66	0	17.94	21.6	3.66	0	3.66	0
AR	0	0	0	0	0	0	0	0	0
CH4	0	0.28	0	0	0	0.28	0	0	0
C2H6	0	0.03	0	0	0	0.03	0	0	0
C2H4	0	0.11	0	0	0	0.11	0	0	0
C6H6	0	0.02	0	0	0	0.02	0	0	0
C3	0	0	0	0	0	0	0	0	0
C4	0	0	0	0	0	0	0	0	0
H2S	0	0	0	0	0	0	0	0	0
NH3	0	0.01	0	0	0	0.01	0	0	0
TAR	0	0.04	0	0	0	0.04	0	0	0
SULFUR	0	0	0	0	0	0	0	0	0
CARBON	0	0	0	0	0	0	0	0	0
STEAM	0	0	0	0	0	0	0	0	0
SO2	0	0	0	0	0	0	0	0	0
NO2	0	0	0	0	0.01	0	0	0	0
MEA	0	0	0	0	0	0	0	0	0
AIR	0	0	0	0	0	0	0	0	0
WAXES	0	0	0	0	0	0	0	0	0
BIOMASS	0	0	4.05	0	0	0	0	0	0
ASH	0.07	0	0	0	0	0.08	0	0	0
CHAR	0.45	0.01	0	0	0.01	0.46	0	0	0

Table C.2 Area 100: Gasification Stream Data

Area 100: Gasification	GS05SGAS	GS08BMAS	GS10BMAS	GS11BMAS	GS12BMAS	GS14BMAS	GS21SGAS	GS90OX	GS91STM	GS92AIR	GS92OXID
Temperature (°C)	815	25	25	25	25	25	815	148.89	204.44	25	29.24
Pressure (bar)	2.25	1.27	1.27	1.27	2.25	2.25	2.25	2.25	22	1.24	22
Vapor Fraction	1	0	0	0	0	0	1	1	0	1	1
Volume Flow ** (m^3/sec)	0.14	0	0	0	0	0	0.14	0	0	0.04	0
Mole Flow ** (kmol/hr)	12.38	0.62	0.62	0.62	0.62	0.62	12.38	0	0	6.7	6.7
Mass Flow (tonnes/day)	8.95	4.32	4.32	4.32	4.32	4.32	8.95	0	0	4.63	4.63
H2O	0.57	0.27	0.27	0.27	0.27	0.27	0.57	0	0	0	0
CO	1.34	0	0	0	0	0	1.34	0	0	0	0
H2	0.02	0	0	0	0	0	0.02	0	0	0	0
CO2	2.35	0	0	0	0	0	2.35	0	0	0	0
O2	0	0	0	0	0	0	0	0	0	0.97	0.97
N2	3.66	0	0	0	0	0	3.66	0	0	3.66	3.66
AR	0	0	0	0	0	0	0	0	0	0	0
CH4	0.28	0	0	0	0	0	0.28	0	0	0	0
C2H6	0.03	0	0	0	0	0	0.03	0	0	0	0
C2H4	0.11	0	0	0	0	0	0.11	0	0	0	0
C6H6	0.02	0	0	0	0	0	0.02	0	0	0	0
C3	0	0	0	0	0	0	0	0	0	0	0
C4	0	0	0	0	0	0	0	0	0	0	0
H2S	0	0	0	0	0	0	0	0	0	0	0
NH3	0.01	0	0	0	0	0	0.01	0	0	0	0
TAR	0.04	0	0	0	0	0	0.04	0	0	0	0
SULFUR	0	0	0	0	0	0	0	0	0	0	0
CARBON	0	0	0	0	0	0	0	0	0	0	0
STEAM	0	0	0	0	0	0	0	0	0	0	0
SO2	0	0	0	0	0	0	0	0	0	0	0
NO2	0	0	0	0	0	0	0	0	0	0	0
MEA	0	0	0	0	0	0	0	0	0	0	0
AIR	0	0	0	0	0	0	0	0	0	0	0
WAXES	0	0	0	0	0	0	0	0	0	0	0
BIOMASS	0	4.05	4.05	4.05	4.05	4.05	0	0	0	0	0
ASH	0.08	0	0	0	0	0	0.08	0	0	0	0
CHAR	0.46	0	0	0	0	0	0.46	0	0	0	0

Table C.3 Area 200 and 300: Gas Cleanup and Combustion Stream Data

Area 200: Gas Cleanup	PL21SGAS	CY01SGAS	CY01CHAR	CY02CHAR	CY05CHAR	CY03SGAS	CY07SGAS	Area 300: Combustion	CB50FLUE	PL07SGAS	CB37AIR
Temperature (°C)	815	350				350	350		1900	350	25
Pressure (bar)	2.25	2.05	2.05	2.05	2.05	2.05	2.05		1.01	2.05	1.01
Vapor Fraction	1	1				1	1		1	1	1
Volume Flow ** (m^3/sec)	0.14	0.09	0	0	0	0.09	0.09		2.23	0.09	0.23
Mole Flow ** (kmol/hr)	12.38	12.38	0	0	0	12.38	12.38		44.97	12.38	33.78
Mass Flow (tonnes/day)	8.95	8.95	0.47	0.06	0.53	8.48	8.42		31.81	8.42	23.39
H2O	0.57	0.57	0	0	0	0.57	0.57		1.62	0.57	0
CO	1.34	1.34	0	0	0	1.34	1.34		0	1.34	0
H2	0.02	0.02	0	0	0	0.02	0.02		0	0.02	0
CO2	2.35	2.35	0	0	0	2.35	2.35		5.85	2.35	0
O2	0	0	0	0	0	0	0		2.72	0	5.45
N2	3.66	3.66	0	0	0	3.66	3.66		21.6	3.66	17.94
AR	0	0	0	0	0	0	0		0	0	0
CH4	0.28	0.28	0	0	0	0.28	0.28		0	0.28	0
C2H6	0.03	0.03	0	0	0	0.03	0.03		0	0.03	0
C2H4	0.11	0.11	0	0	0	0.11	0.11		0	0.11	0
C6H6	0.02	0.02	0	0	0	0.02	0.02		0	0.02	0
C3	0	0	0	0	0	0	0		0	0	0
C4	0	0	0	0	0	0	0		0	0	0
H2S	0	0	0	0	0	0	0		0	0	0
NH3	0.01	0.01	0	0	0	0.01	0.01		0	0.01	0
TAR	0.04	0.04	0	0	0	0.04	0.04		0	0.04	0
SULFUR	0	0	0	0	0	0	0		0	0	0
CARBON	0	0	0	0	0	0	0		0	0	0
STEAM	0	0	0	0	0	0	0		0	0	0
SO2	0	0	0	0	0	0	0		0	0	0
NO2	0	0	0	0	0	0	0		0.01	0	0
MEA	0	0	0	0	0	0	0		0	0	0
AIR	0	0	0	0	0	0	0		0	0	0
WAXES	0	0	0	0	0	0	0		0	0	0
BIOMASS	0	0	0	0	0	0	0		0	0	0
ASH	0.08	0.08	0.07	0.01	0.07	0.01	0		0	0	0
CHAR	0.46	0.46	0.4	0.05	0.45	0.05	0.01		0.01	0.01	0

APPENDIX D. ENGINEERING EQUATION SOLVER (EES) CODE

The following code is used to calculate the adiabatic flame temperature of the producer gas with zero ammonia and an equivalence ratio of 2. This code can be manipulated to handle different gas compositions and equivalence ratios.

```
"Tr = reactant temperature (C)
Tp = prodct temperature (C)
hr = reactant enthalpy (kJ/kmol)
hp = product enthalpy (kJ/kmol)
atom balances and first law of thermodynamics is used to find adiabatic flame temperature
"n3CH4 + n1CO + n2H2 + n4C2H2 + n5C2H4 + n6C2H6 + n7C3H8 + n8NH3 + nN2+ nCO2 a(O2 + 3.76N2) -> bCO2 + cH2O + dN2"

GasificationPhi = 2
Phi = 1/GasificationPhi

"Composition”

nCH4 = 0.0586
nCO =0.194
nH2 = 0.1269
nNH3 = 0.0
nN2 = 0.448
nCO2 = .155
nC2H6 = .0028
nC2H4 = .0131
nC2H2 = .0008
nC3H8 = .0008

"Atom Balance”
astoich=(nH2 + nCO + 4*nCH4 + 7*nC2H6 + 6*nC2H4 + 5*nC2H2 + 10*nC3H8 + 1.5*nNH3)/2
b = nCH4 + nCO + nCO2 +2*nC2H6 + 2*nC2H4 + 2*nC2H2 + 3*nC3H8
c = (2*nH2 +4*nCH4 +6*nC2H6 + 4*nC2H4 +2*nC2H2 + 8*nC3H8 + 3* nNH3)/2
d = .5* nNH3 + 3.76*a +nN2
f = max(0, a-astoich)

"Reactant Properties”
a = astoich/Phi
Treac = 25

"Enthalpies”
hrCH4 = ENTHALPY(CH4, T = Treac)
hrCO = ENTHALPY(CO, T=Treac)
hrH2 = ENTHALPY(H2, T=Treac)
hrNH3 = ENTHALPY(NH3, T=Treac)
hrO2 = ENTHALPY(O2, T=Treac)
hrN2 = ENTHALPY(N2, T=Treac)
hrCO2 = ENTHALPY(CO2, T=Treac)
hrC2H6 = ENTHALPY(C2H6, T=Treac)
hrC2H4 = ENTHALPY(C2H4,T=Treac)
hrC2H2 = ENTHALPY(C2H2, T=Treac)
```

```
hrC3H8 = ENTHALPY(C3H8, T=Treac)
hpCO2 = ENTHALPY(CO2, T = Tprod)
hpH2O = ENTHALPY(H2O, T = Tprod)
hpO2 = ENTHALPY(O2, T = Tprod)
hpN2 = ENTHALPY(N2, T = Tprod)

hrefCO2=ENTHALPY(CO2,T=Tr)
hrefH2O=ENTHALPY(H2O,T=Tr)
hrefN2=ENTHALPY(N2,T=Tr)

"Net reactant enthalpy"
h_ reac = nCH4*hrCH4 + nCO*hrCO + nH2*hrH2 + nNH3*hrNH3 + a*hrO2 + (3.76*a+nN2)*hrN2 +
nCO2*hrCO2 + nC2H6*hrC2H6 + nC2H4*hrC2H4 + nC2H2*hrC2H2 + nC3H8*hrC3H8

"Energy Balance"
h_reac= b*hpCO2 + c*hpH2O + f*hpO2 + (d)*hpN2

"Lower heating value calculation"
LHV = h_reac - (d*hrefN2+b*hrefCO2+c*hrefH2O)
```